NASA TECHNICAL MEMORANDUM

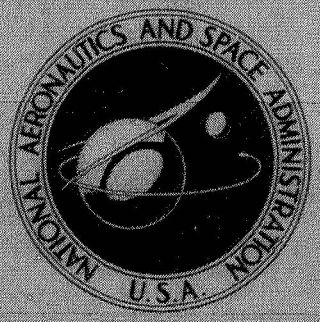

NASA TM X-1998

NASA TM X-1998

LOW SUBSONIC AERODYNAMIC CHARACTERISTICS OF A MEDIUM HYPERSONIC L/D REENTRY SPACECRAFT WITH A VARIABLE GEOMETRY WING

by John P. Decker and Bernard Spencer, Jr.

Langley Research Center
Langley Station, Hampton, Va.

NATIONAL AERONAUTICS AND SPACE ADMINISTRATION • WASHINGTON, D. C. • APRIL 1970

1. Report No. NASA TM X-1998	2. Government Accession No.	3. Recipient's Catalog No.
4. Title and Subtitle LOW SUBSONIC AERODYNAMIC CHARACTERISTICS OF A MEDIUM HYPERSONIC L/D REENTRY SPACECRAFT WITH A VARIABLE GEOMETRY WING		5. Report Date April 1970 6. Performing Organization Code
7. Author(s) John P. Decker and Bernard Spencer, Jr.		8. Performing Organization Report No. L-6945 10. Work Unit No. 124-64-01-03-23
9. Performing Organization Name and Address NASA Langley Research Center Hampton, Va. 23365		11. Contract or Grant No. 13. Type of Report and Period Covered Technical Memorandum
12. Sponsoring Agency Name and Address National Aeronautics and Space Administration Washington, D.C. 20546		14. Sponsoring Agency Code

15. Supplementary Notes

16. Abstract

A wind-tunnel investigation was conducted at low subsonic Mach numbers between 0.21 and 0.41 and at Reynolds numbers based on body length from about 4.9×10^6 to 29.5×10^6 to determine the basic longitudinal aerodynamic characteristics of a variable geometry spacecraft having a hypersonic lift-drag ratio near 2. The configuration represents one approach to improving the subsonic lift-drag ratio of a lifting body by incorporation of severe afterbody boattailing to decrease the base drag and by the addition of an internally stowed variable-sweep rigid wing. The model was tested with the wings deployed to 20^0 and 90^0 (stowed) at angles of attack from about -6^0 to 16^0.

17. Key Words Suggested by Author(s) Variable geometry spacecraft Lifting bodies	18. Distribution Statement Unclassified – Unlimited		
19. Security Classif. (of this report) Unclassified	20. Security Classif. (of this page) Unclassified	21. No. of Pages 39	22. Price* $3.00

*For sale by the Clearinghouse for Federal Scientific and Technical Information Springfield, Virginia 22151

LOW SUBSONIC AERODYNAMIC CHARACTERISTICS OF A MEDIUM HYPERSONIC L/D REENTRY SPACECRAFT WITH A VARIABLE GEOMETRY WING

By John P. Decker and Bernard Spencer, Jr.
Langley Research Center

SUMMARY

A wind-tunnel investigation was conducted at low subsonic Mach numbers between 0.21 and 0.41 and at Reynolds numbers based on body length from 4.9×10^6 to 29.5×10^6 to determine the longitudinal aerodynamic characteristics of a variable geometry spacecraft having a hypersonic lift-drag ratio near 2. The configuration represents one approach to improving the subsonic lift-drag ratio of a lifting body by incorporation of severe afterbody boattailing to decrease the base drag and by the addition of an internally stowed variable-sweep rigid wing. The model was tested with the wings deployed to 20° and 90° (stowed) at angles of attack from about -6° to 16°.

The results of the investigation indicated that increasing the Reynolds number on the model with the wings stowed had essentially no effect on the longitudinal aerodynamic characteristics. Increasing the Reynolds number on the model with wings deployed to 20° increased the lift coefficient for the onset of flow separation but did not linearize the pitching-moment curves and the configuration remained neutrally stable or statically unstable at higher lift coefficients; no significant improvement in maximum lift-drag ratio was indicated as the Reynolds number was increased from 4.9×10^6 to 29.3×10^6. The spacecraft with the wings stowed or deployed to 20° required a large negative deflection of the elevons to trim at any reasonable lift coefficient, and hence a large reduction in maximum lift-drag ratio resulted.

INTRODUCTION

The National Aeronautics and Space Administration is presently conducting investigations on reentry spacecraft which employ variable geometry wings for horizontal-landing capability. One such vehicle having a hypersonic lift-drag ratio of about 2 has been tested at transonic speeds. (See ref. 1.) As a continuation of this investigation, tests have been conducted in the Langley low-turbulence pressure tunnel at Mach numbers representative of landing.

The configuration represents one approach to improving the subsonic lift-drag ratio of a lifting body by incorporation of severe afterbody boattailing to decrease the base drag and by the addition of an internally stowed variable-sweep rigid wing. Aerodynamic control surfaces, located at the trailing edge on the top and bottom of the body, may function in unison at subsonic speeds to minimize base drag, or independently at higher speeds where base drag is of less significance. The wing, of rectangular planform and positioned so that it would be stowed inside of the spacecraft just above the lower surface heat shield, was sized to maximize the useful wing area in subsonic flight. For landing, the wing would be deployed to a low sweep position. This present configuration design philosophy was derived primarily from the baseline vehicle described in reference 2.

The spacecraft was tested with the wings deployed to 20° and 90° (stowed) at Mach numbers varying between 0.21 and 0.41. The Reynolds number based on body length was varied from 4.9×10^6 to 29.5×10^6.

SYMBOLS

The aerodynamic coefficients presented herein are referred to the body axes system with the exception of the lift and drag coefficients which are referred to the stability axes system. The moment reference center was located at 50 percent of the body length along the model reference line. (See fig. 1.) All coefficients are based on the planform area, length, and span of the body alone.

b	body span, 0.1668 m (0.5473 ft)
C_D	drag coefficient, $\frac{\text{Drag}}{qS}$
C_L	lift coefficient, $\frac{\text{Lift}}{qS}$
C_l	rolling-moment coefficient, $\frac{\text{Rolling moment}}{qSb}$
C_m	pitching-moment coefficient, $\frac{\text{Pitching moment}}{qSl}$
$C_{m,o}$	pitching-moment coefficient at $C_L = 0$
C_n	yawing-moment coefficient, $\frac{\text{Yawing moment}}{qSb}$
C_Y	side-force coefficient, $\frac{\text{Side force}}{qS}$
L/D	lift-drag ratio

$(L/D)_{max}$ maximum lift-drag ratio

l body length, 0.6568 m (2.155 ft)

M free-stream Mach number

q free-stream dynamic pressure

R Reynolds number based on body length

S body projected planform area, 0.08542 m^2 (0.91944 ft^2)

α angle of attack referenced to body axis (see fig. 1), deg

β angle of sideslip, deg

$\delta_{e,l}$ lower elevon deflection (fig. 1) positive for trailing edge down, deg

$\delta_{e,u}$ upper elevon deflection (fig. 1) positive for trailing edge down, deg

Λ wing leading-edge sweep angle, deg

APPARATUS AND METHODS

Model

Details of the model which was identical to the model of reference 1 are shown in figure 1. Geometric characteristics of the model are shown in table I. The basic spacecraft had cross-sectional shape progressions as indicated in figure 1 and was provided with two outboard mounted vertical tails which had a cant angle of 13° and a toe-in angle of 11.5°. The spacecraft had afterbody boattailing to reduce the base drag at subsonic speeds and was provided with upper and lower elevons located near the base of the spacecraft. The spacecraft was tested with upper surface boattail angles of approximately 12° (original), 9°, and 6°.

The model was also provided with a deployable low wing which had a constant chord perpendicular to the leading edge and an incidence angle of 5° when at a 0° sweep position. The airfoil was a modified NACA 64_3-618 section. The wing was tested at sweep angles of 20° and 90° (stowed). Some photographs of the model are shown as figure 2.

Tunnel

The tests were conducted in the Langley low-turbulence pressure tunnel which is a variable-pressure, single-return facility having a closed test section. The tunnel can accommodate tests in air at Reynolds numbers per foot (per meter) from 1.0×10^6 (3.3×10^6) to 15.0×10^6 (49.2×10^6) at Mach numbers up to about 0.40.

Test Conditions

The tests were conducted at Mach numbers between 0.21 and 0.41. The angle of attack was varied from about -6° to 16° at an angle of sideslip of 0°. Tests were made with and without artificial transition strips. The tests with the transition strips on the model were used for comparison of data obtained in reference 1 at $M = 0.40$. For the tests with transition strips on the model, a 0.05-inch-wide (0.13-cm) band of No. 120 (0.0049-in. or 0.0124-cm) carborundum grit was located 0.80 in. (2.03 cm) streamwise behind the forebody apex and vertical tails and 0.60 in. (1.52 cm) streamwise behind the wing leading edge. For some of the runs, the entire lower surface of the body was covered with a sparse coating of No. 80 (0.0083-in. or 0.0211-cm) carborundum grit to obtain some information on the effect of ablation surface roughness.

Model Support, Measurements, and Corrections

The model was sting supported and the aerodynamic forces and moments were measured by an internally mounted six-component strain-gage balance. When the lower elevon was deflected to -15°, part of the sting forward of the base was exposed to the airstream. (See fig. 3(a).) Reference 1 presented data with a fairing over the exposed part of the sting (fig. 3(b)) on and off. Consequently, in the present investigation only data with the lower elevon fairing on are presented.

Balance chamber and elevon base pressures were measured by means of static orifices located in the balance chamber and at the base of the elevons. However, no base drag corrections were applied to the data. No sting interference corrections have been applied to the data although some small interference effects probably are present. Angles of attack were corrected for balance and sting deflection due to aerodynamic loading. No corrections were made for tunnel flow misalinement, jet boundary, or tunnel blockage. However, one run was made at a Mach number of 0.41 to compare with data obtained in reference 1.

PRESENTATION OF RESULTS

The results of the investigation are presented in the following figures:

DISCUSSION

Data Comparison

Figure 4 presents data obtained in the present investigation with data obtained in reference 1 at corresponding Mach numbers and Reynolds numbers. Good agreement in the data curves is shown at angles below the onset of flow separation. Hence, any flow misalinement, jet boundary, or tunnel blockage corrections appear to be within the accuracy of the data and therefore no corrections have been applied.

Effect of Reynolds Number

Increasing the Reynolds number from 4.9×10^6 to 29.3×10^6 on the model with the wings stowed ($\Lambda = 90^{o}$) (fig. 5) had essentially no effect on the longitudinal aerodynamic characteristics. However, increasing the Reynolds number on the model with the wings deployed to $\Lambda = 20^{o}$ (fig. 6) linearized the lift-curve slope and extended the usable lift coefficient prior to the onset of flow separation on the wings. Increasing Reynolds number did not however linearize the pitching-moment curve and the configuration remains neutrally stable or statically unstable at lift coefficients near $(L/D)_{max}$. The sudden pitch-up has however been delayed to higher angles of attack and lift coefficients by increasing Reynolds number. Figure 6 also indicates no significant improvement in $(L/D)_{max}$ as the Reynolds number is increased from 4.9×10^6 to 29.3×10^6; however, the lift coefficient at which $(L/D)_{max}$ occurs increased by about 0.10.

Effect of Elevon Deflections

Figure 7 indicates that a large negative deflection of the elevons is required to trim out the negative $C_{m,o}$ shown for the model with the wings stowed ($\Lambda = 90^o$ with fully boattailed afterbody) and elevons set at 0^o. Figure 7 includes data at other elevon settings with the wings stowed and indicates that a large negative deflection of both the upper and lower elevons would be required to trim at moderate lift coefficients; as a result, there is a substantial loss in $(L/D)_{max}$. The reason for this loss in $(L/D)_{max}$ is twofold. First, if the lower elevon is deflected to a large negative angle, flow separation would be expected to occur on the lower elevon surface and thereby the drag would be increased. Secondly, deflection of the upper elevon increases the base area and, consequently, the base drag. Hence, the loss in $(L/D)_{max}$ indicated in figure 7 due to deflection of the lower and upper elevons appears to be reasonable. However, a complete analysis of the drag increments due to elevon deflections would be required to determine the actual trimmed $(L/D)_{max}$; such an analyses is beyond the scope of this paper. Figure 7 also indicates that the deflection of the upper elevon produces a destabilizing increment to the longitudinal stability.

With the wings deployed to 20^o, figure 8 indicates that the wings increased the negative C_m at $\alpha = 0^o$ (compare fig. 8 with fig. 7 at $\alpha = 0^o$) and that a large negative deflection of the elevons is also required to trim the vehicle to any reasonable C_L; as a result, large reductions in $(L/D)_{max}$ were obtained. At lift coefficients for $(L/D)_{max}$, the stability level has decreased to essentially zero or slightly unstable for nearly all deflections, either upper or lower, of the elevons.

Effect of Reduced Body Boattail

To understand better the $C_{m,o}$ problem, that is, the large negative $C_{m,o}$ that has to be overcome to trim the vehicle at a positive C_L, a series of body boattail angles were investigated. (See fig. 1 for boattail description.) Figure 9 presents the results for the basic spacecraft ($\Lambda = 90^o$) and indicates that reducing the boattail angle from 12^o to 6^o provides a small positive $C_{m,o}$ increment and a decrease in the static longitudinal stability. However, comparison of the data in figure 9 with the data for the various elevon deflections in figure 7 indicates that reflexing the trailing edge of the spacecraft is more effective than reducing the boattail angle of the basic spacecraft. Compare, for example, the $C_{m,o}$ increment due to $\delta_{e,u} = -35^o$ with the $C_{m,o}$ increment due to reducing the boattail angle from 12^o to 6^o.

Figure 10 presents the results for the model with the wings deployed to $\Lambda = 20^o$ and indicates similar results for the basic spacecraft with the wings stowed. Both figure 10 and figure 9 indicate a large drag increase due to reducing the boattail angle from 12^o to 6^o and consequently a large reduction in untrimmed L/D.

Figure 11 presents the control effectiveness for the model with a boattail angle of 6^{o} and wings stowed. Comparison of the data in figure 11 with the data in figure 7 indicates that the $C_{m,o}$ increment due to elevon deflection is about the same for both configurations.

Effect of Ablation Surface Roughness

Figure 12 presents results for the basic spacecraft ($\Lambda = 90^{o}$) where an attempt has been made to quantify the effects of ablation surface roughness. For these tests, a sparse coating of No. 80 (0.0083-in. or 0.0211-cm) carborundum grit was applied over the flat portion of the lower surface. The tests were conducted for a Reynolds number from 5.5×10^{6} to 29.5×10^{6} and the data indicate that the roughness caused an expected increase in C_{D} with a small reduction in untrimmed $(L/D)_{max}$. There are not, however, any changes in the static stability characteristics of the spacecraft.

SUMMARY OF RESULTS

Wind-tunnel tests to determine the longitudinal aerodynamic characteristics of a variable geometry spacecraft at low subsonic speeds and at Reynolds numbers, based on body length, from 4.9×10^{6} to 29.5×10^{6} have indicated the following results:

1. Increasing the Reynolds number on the basic spacecraft with the wings stowed has essentially no effect on the longitudinal aerodynamic characteristics.

2. Increasing the Reynolds number on the basic spacecraft with wings deployed to 20^{o} increases the lift coefficient for the onset of flow separation but does not linearize the pitching-moment curves and the configuration remains neutrally stable or statically unstable at higher lift coefficients; no significant improvement in maximum lift-drag ratio was indicated as the Reynolds number was increased from 4.9×10^{6} to 29.3×10^{6}.

3. The basic spacecraft with the wings stowed or deployed to 20^{o} requires a large negative deflection of the elevons to trim at any reasonable lift coefficient and hence a large reduction in maximum lift-drag ratio results.

4. Reducing the body boattail angle from 12^{o} to 6^{o} provides a small positive pitching-moment-coefficient increment at zero lift and a decrease in the longitudinal stability. However, reflexing the trailing edge of the spacecraft by deflecting the elevons is more effective than reducing the boattail angle.

Langley Research Center,
National Aeronautics and Space Administration,
Langley Station, Hampton, Va., January 30, 1970.

REFERENCES

1. Decker, John P.: Transonic Aerodynamic Characteristics of a Medium Hypersonic L/D Reentry Spacecraft With a Variable Geometry Wing. NASA TM X-1995, 1970.

2. Lynch, Robert A.: The First Manned Lifting Entry Vehicle Configuration. AIAA Pap. No. 66-959, Nov.-Dec. 1966.

TABLE I.- GEOMETRIC CHARACTERISTICS OF MODEL

Body reference dimensions:	
Length, cm (in.)	65.684 (25.860)
Span, cm (in.)	16.683 (6.568)
Area, cm^2 (in^2)	854.185 (132.399)
Body:	
Length, cm (in.)	65.684 (25.860)
Plan area (without fins), cm^2 (in^2)	854.185 (132.399)
Width (without fins), cm (in.)	16.683 (6.568)
Outboard vertical fin:	
Airfoil	Slab
Area (true, per fin), cm^2 (in^2)	69.742 (10.810)
Dihedral (angle with respect to vertical), deg	13.0
Incidence (leading edge toed in), deg	11.5
Leading-edge sweep (projected side view), deg	60.5
Root chord (theoretical), cm (in.)	16.078 (6.330)
Tip chord (theoretical), cm (in.)	4.470 (1.760)
Span (root to tip chord), cm (in.)	9.652 (3.800)
Upper flap:	
Area (reference), cm^2 (in^2)	85.806 (13.300)
Chord (reference), cm (in.)	6.706 (2.640)
Span (reference), cm (in.)	12.802 (5.040)
Hinge-line sweep, deg	0
Lower flap:	
Area (reference), cm^2 (in^2)	85.806 (13.300)
Chord (reference), cm (in.)	6.706 (2.640)
Span (reference), cm (in.)	12.802 (5.040)
Hinge-line sweep, deg	0
Wing:	
Airfoil	Modified 64_3-618
Planform shape	Rectangular
Incidence angle ($\Lambda = 0^o$), deg	5
Exposed area, cm^2 (in^2), at –	
$\Lambda = 20^o$	239.690 (37.152)
$\Lambda = 65^o$	173.264 (26.856)
$\Lambda = 75^o$	94.761 (14.688)
Elevon base areas, cm^2 (in^2), for –	
$\delta_{e,l} = 0^o$; $\delta_{e,u} = 0^o$	39.484 (6.120)
$\delta_{e,l} = -15^o$; $\delta_{e,u} = 0^o$	20.129 (3.120)
$\delta_{e,l} = -15^o$; $\delta_{e,u} = -10^o$	35.871 (5.560)
$\delta_{e,l} = -15^o$ (faired); $\delta_{e,u} = -25^o$	58.839 (9.120)

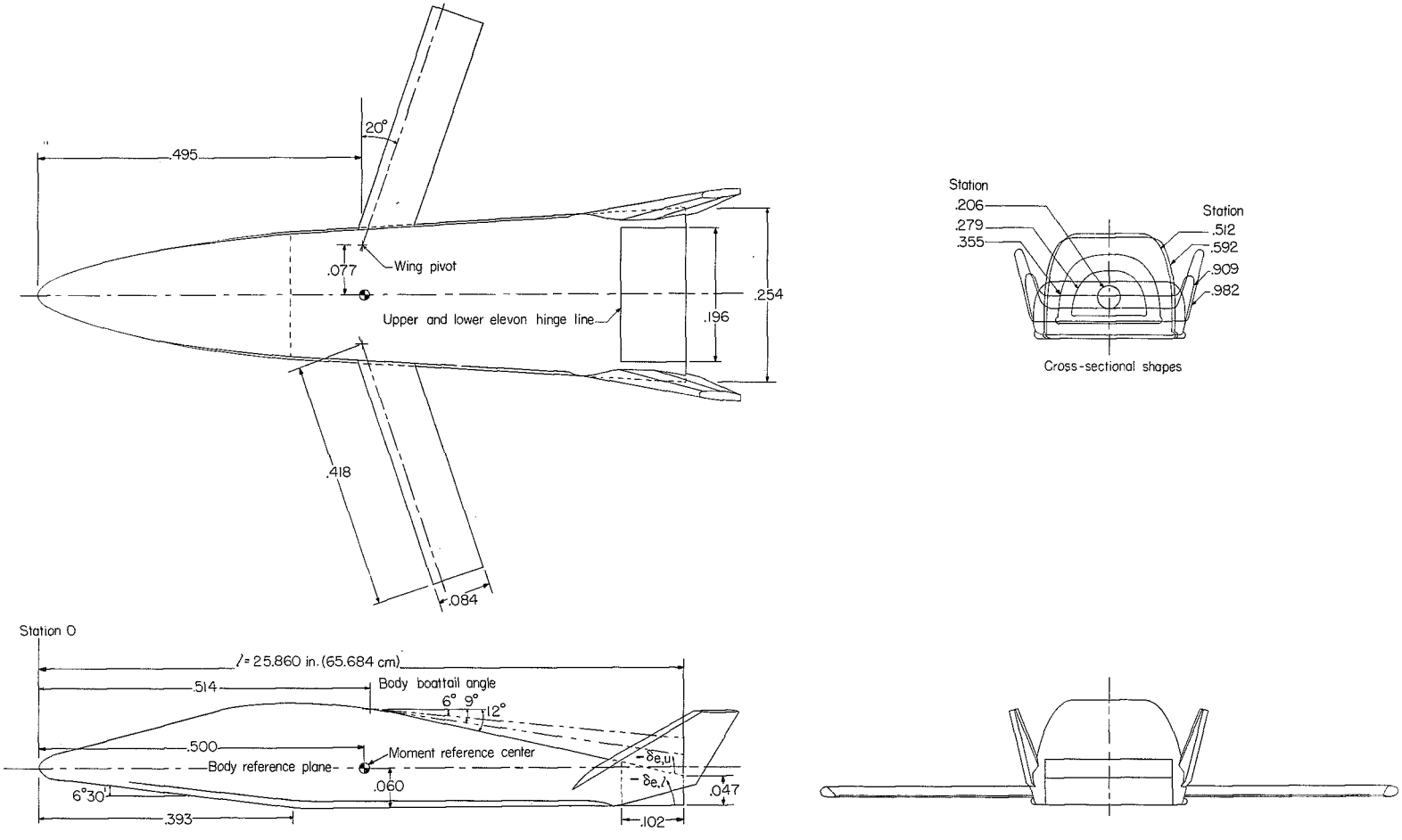

Figure 1.- Details of model. Linear dimensions are based on body length l = 25.860 in. (65.684 cm).

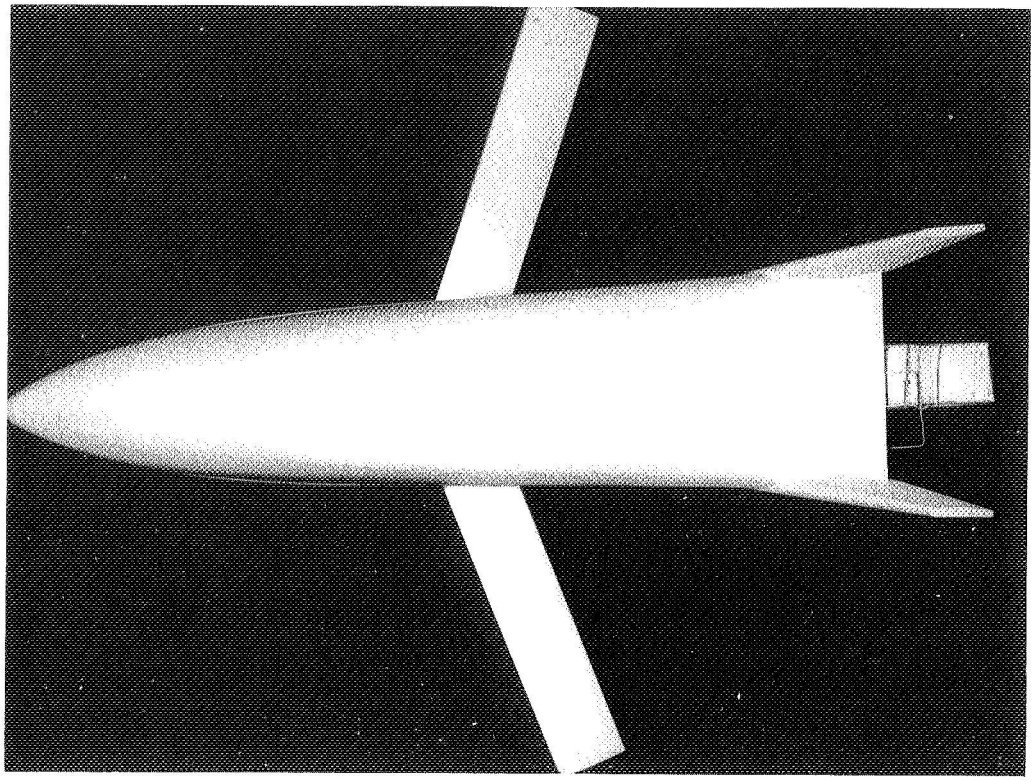

(a) Top view. L-68-3342

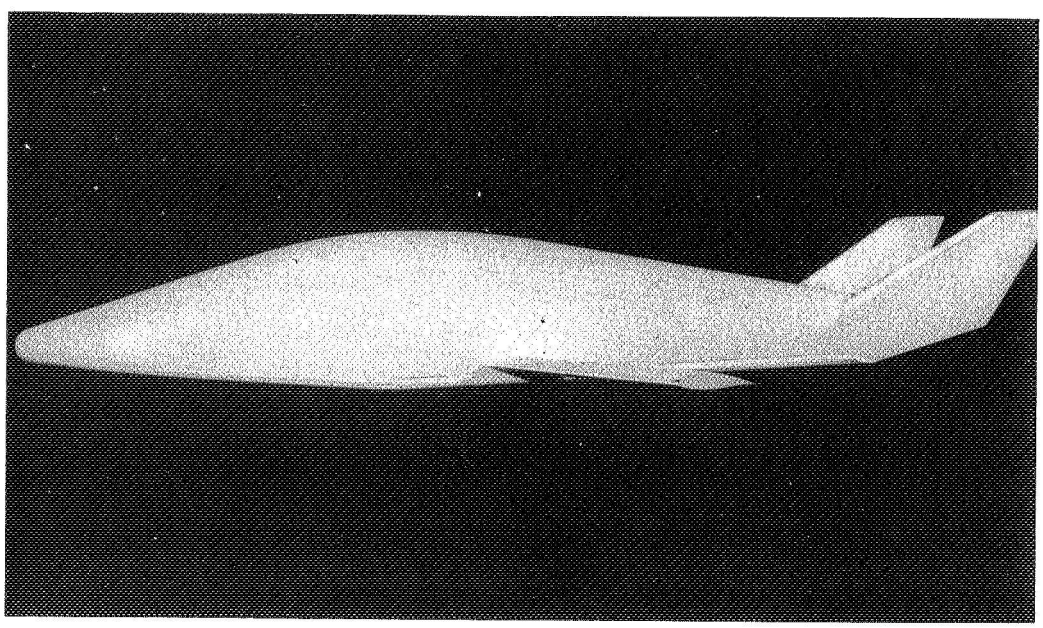

(b) Side view. L-68-3341

Figure 2.- Photographs of model.

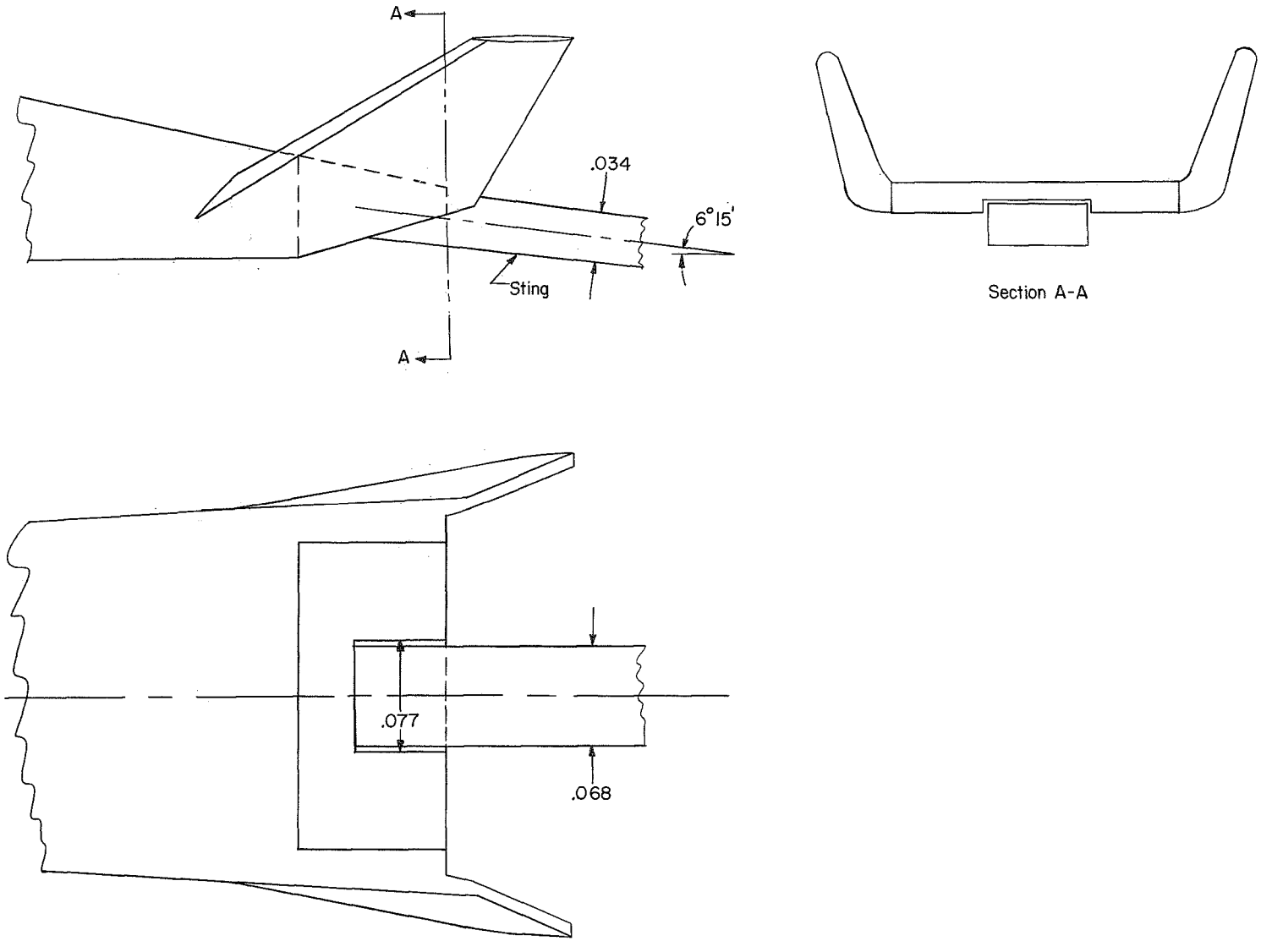

(a) Unfaired lower elevon.

Figure 3.- Modifications to body for sting support when lower elevon is deflected to -15°. All linear dimensions are based on body length ℓ = 25.860 in. (65.680 cm).

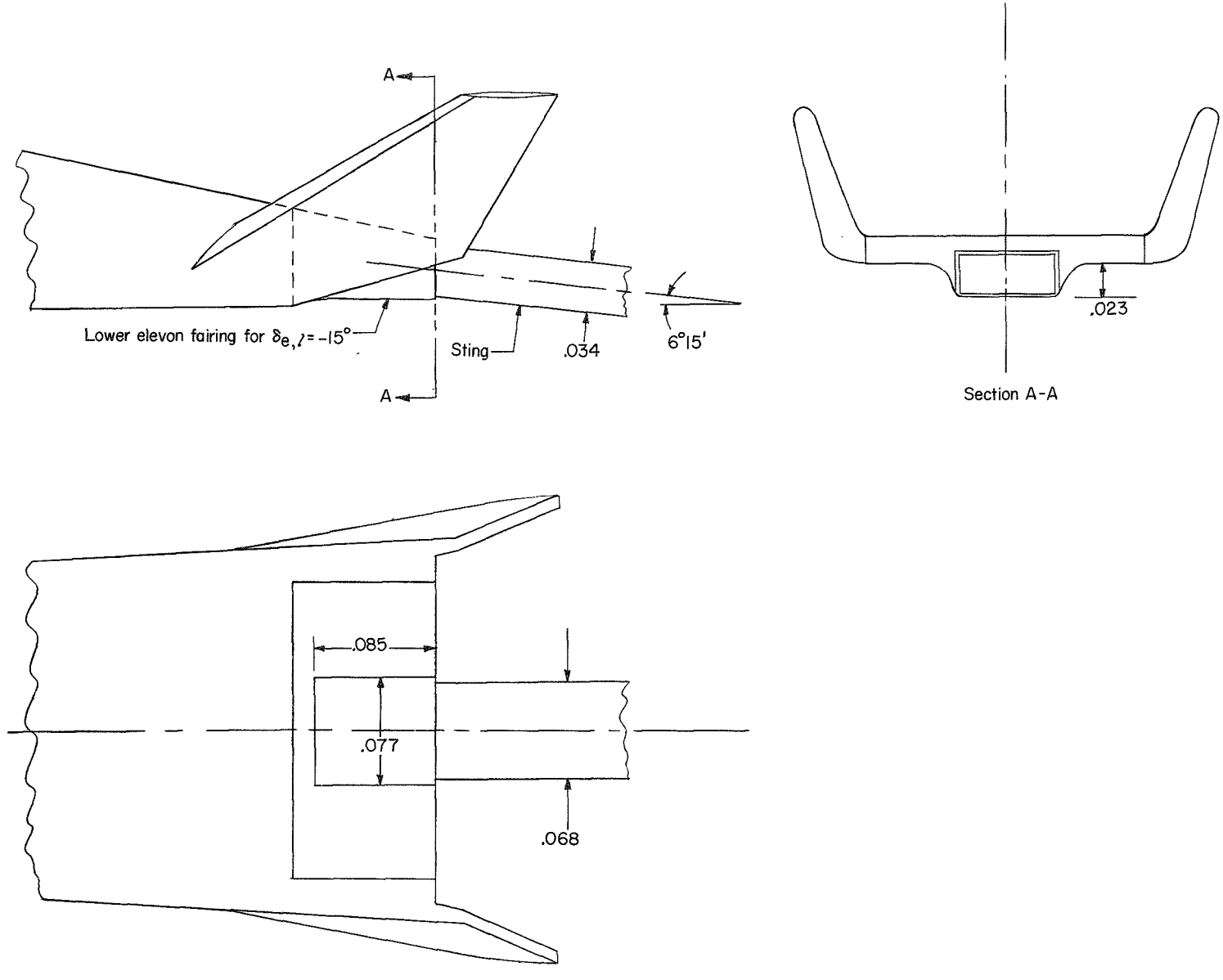

(b) Faired lower elevon.

Figure 3.- Concluded.

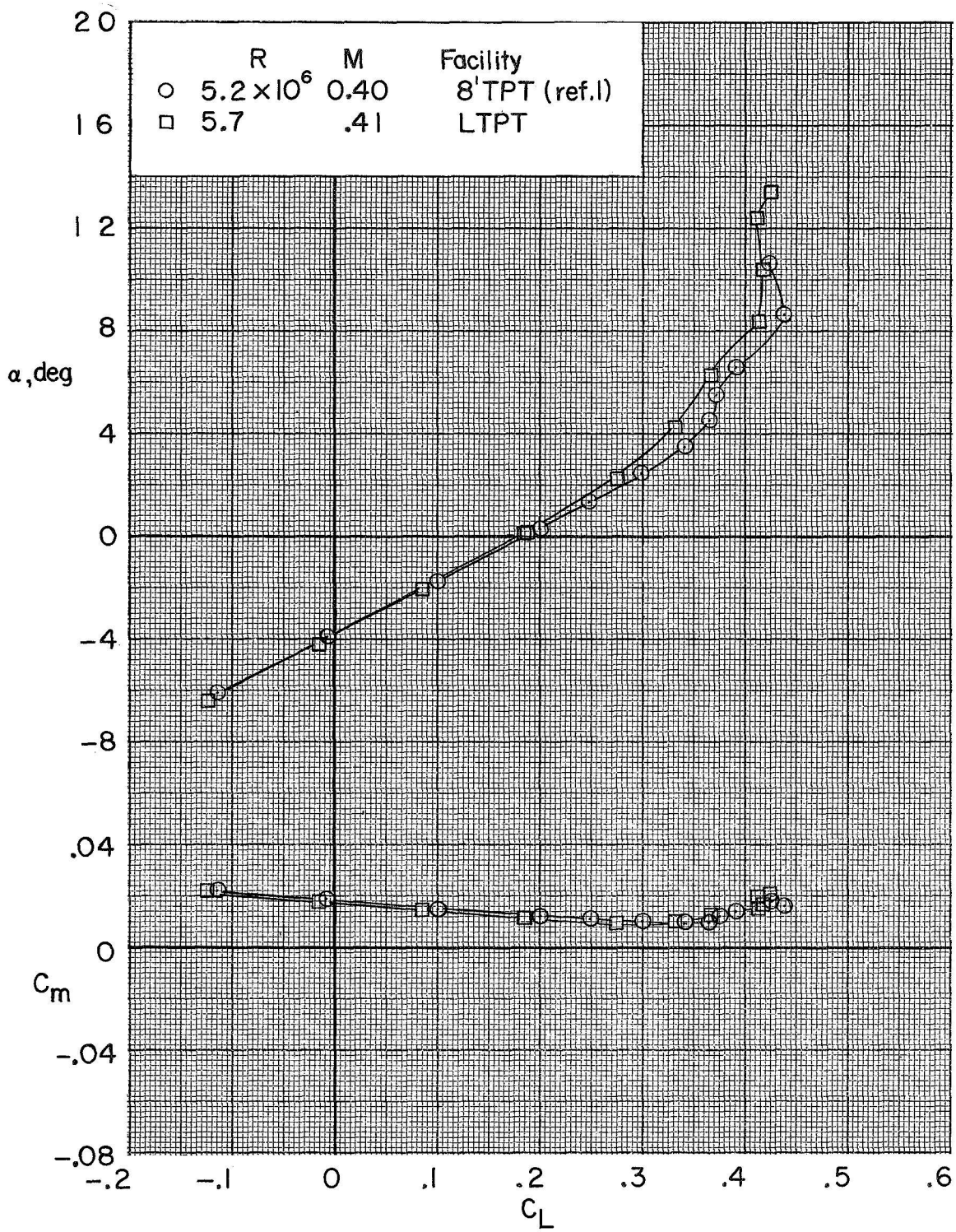

Figure 4.- Comparison of data obtained in the Langley 8-foot transonic pressure tunnel (8'TPT) and the Langley low turbulence pressure tunnel (LTPT) on the model with wings deployed to $\Lambda = 20^0$. $\delta_{e,l} = -15^0$ (faired); $\delta_{e,u} = -25^0$; transition fixed.

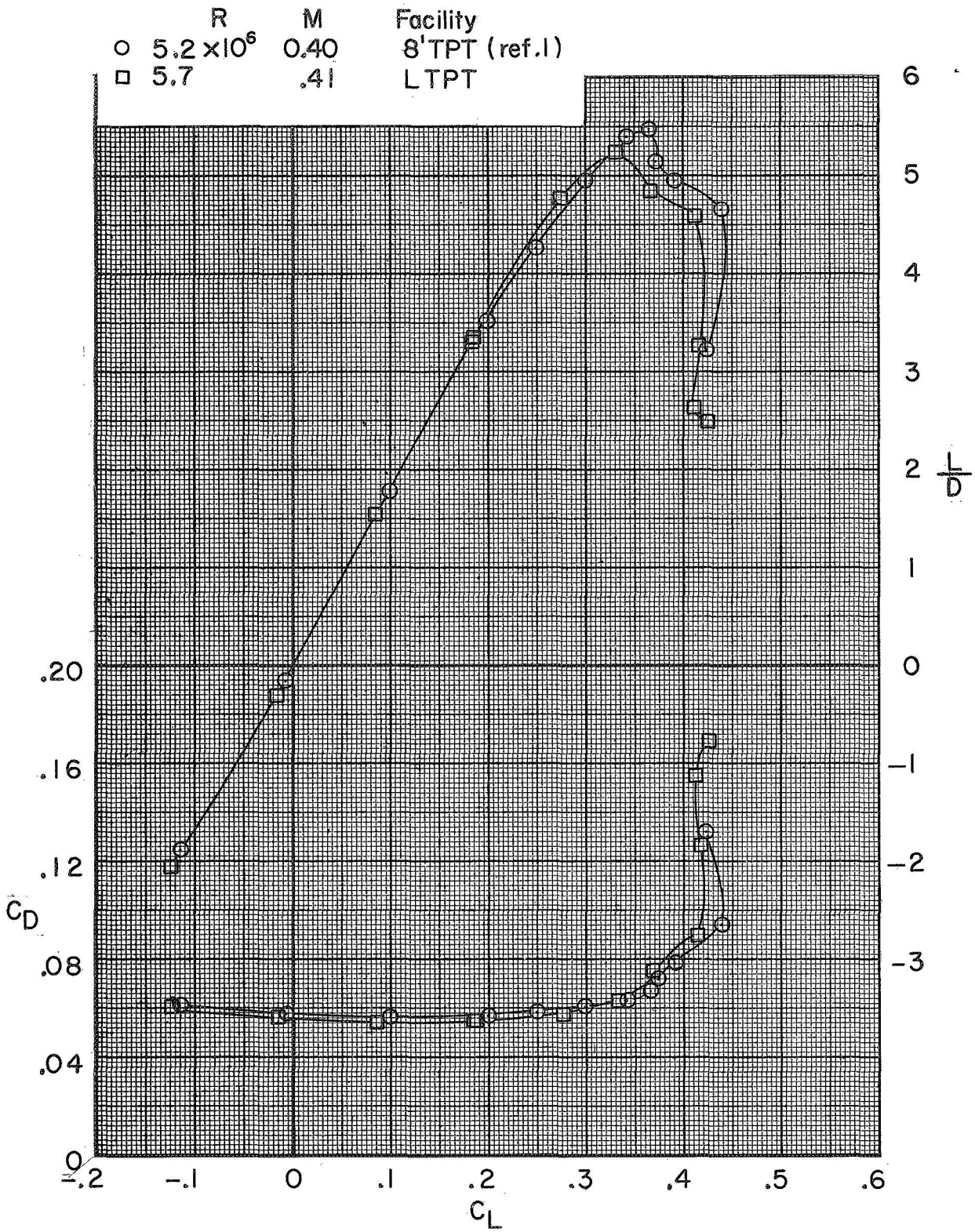

Figure 4.- Concluded.

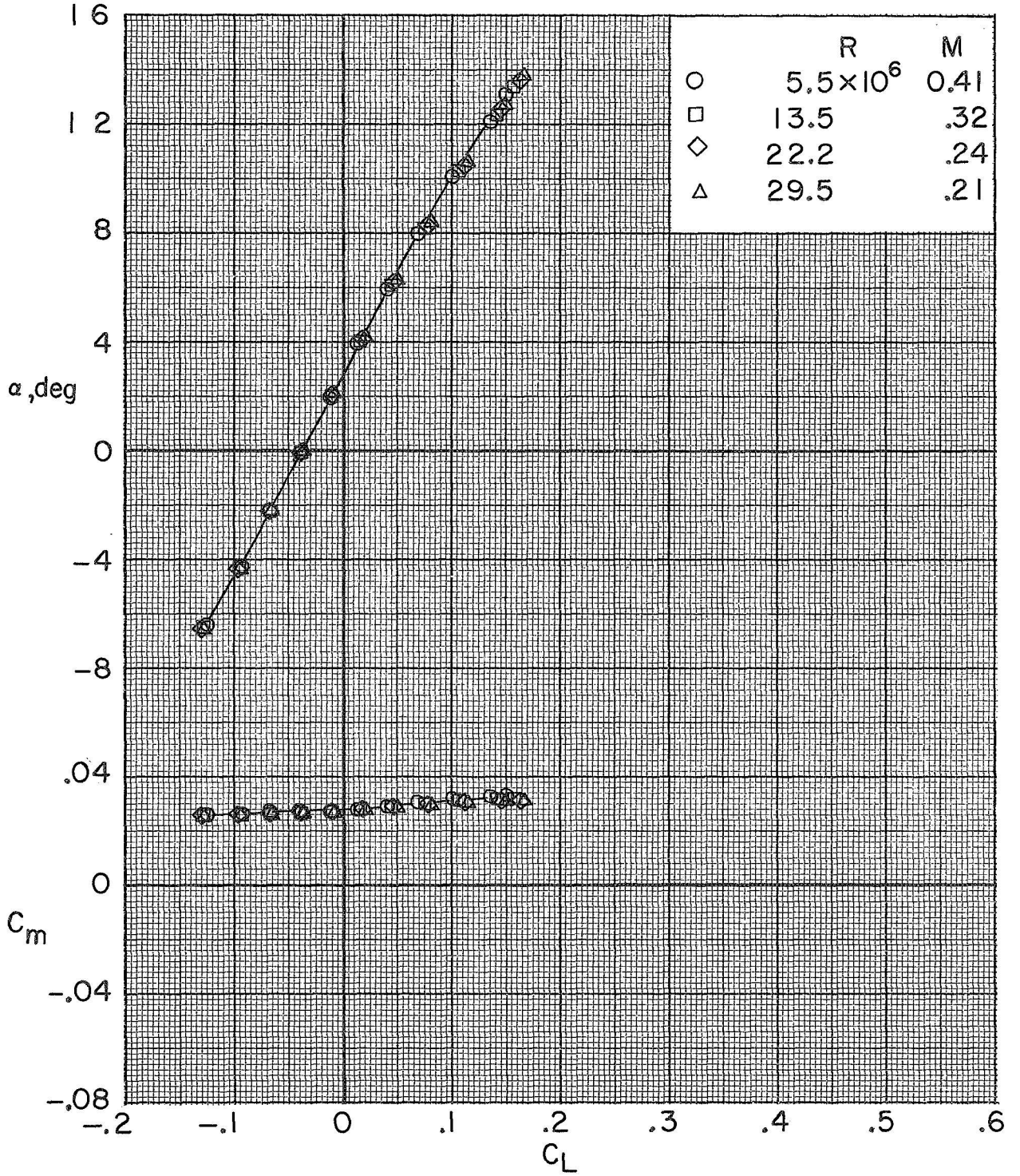

Figure 5.- Effect of Reynolds number on the longitudinal aerodynamic characteristics of the model with wings stowed ($\Lambda = 90^0$). $\delta_{e,l} = -15^0$ (faired); $\delta_{e,u} = -25^0$.

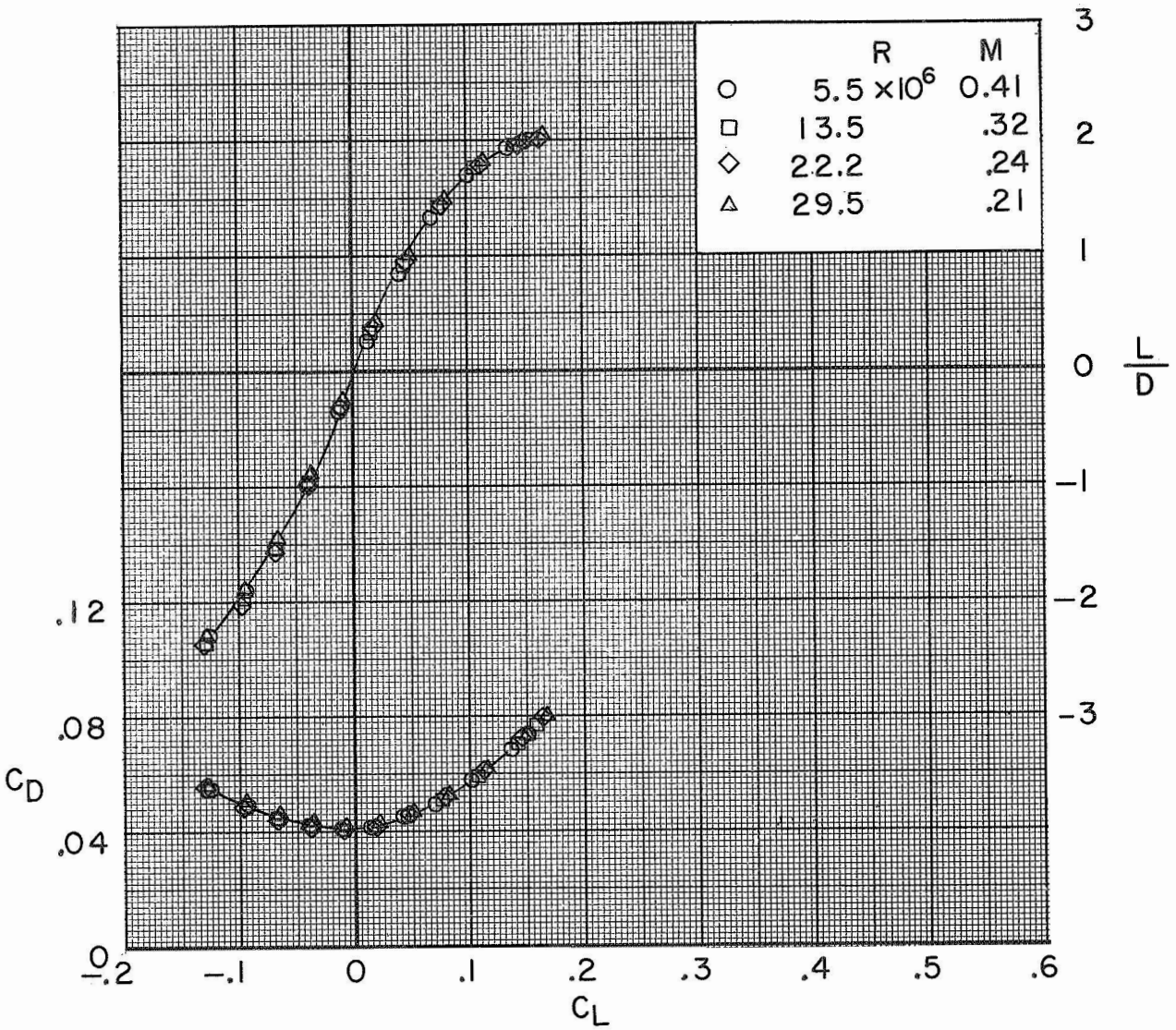

Figure 5.- Concluded.

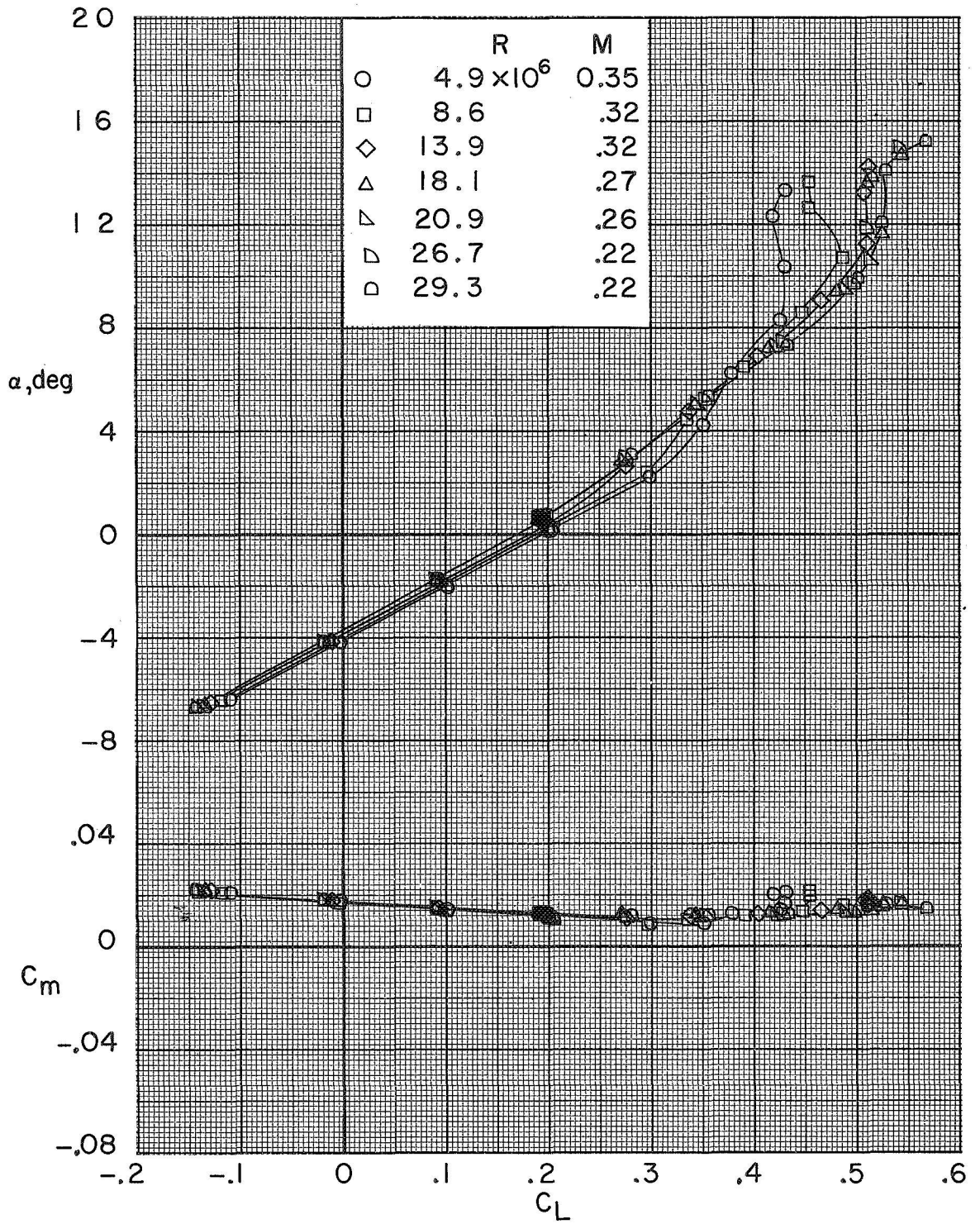

Figure 6.- Effect of Reynolds number on the longitudinal aerodynamic characteristics of the model with wings deployed to $\Lambda = 20^{\circ}$. $\delta_{e,l} = -15^{\circ}$ (faired); $\delta_{e,u} = -25^{\circ}$.

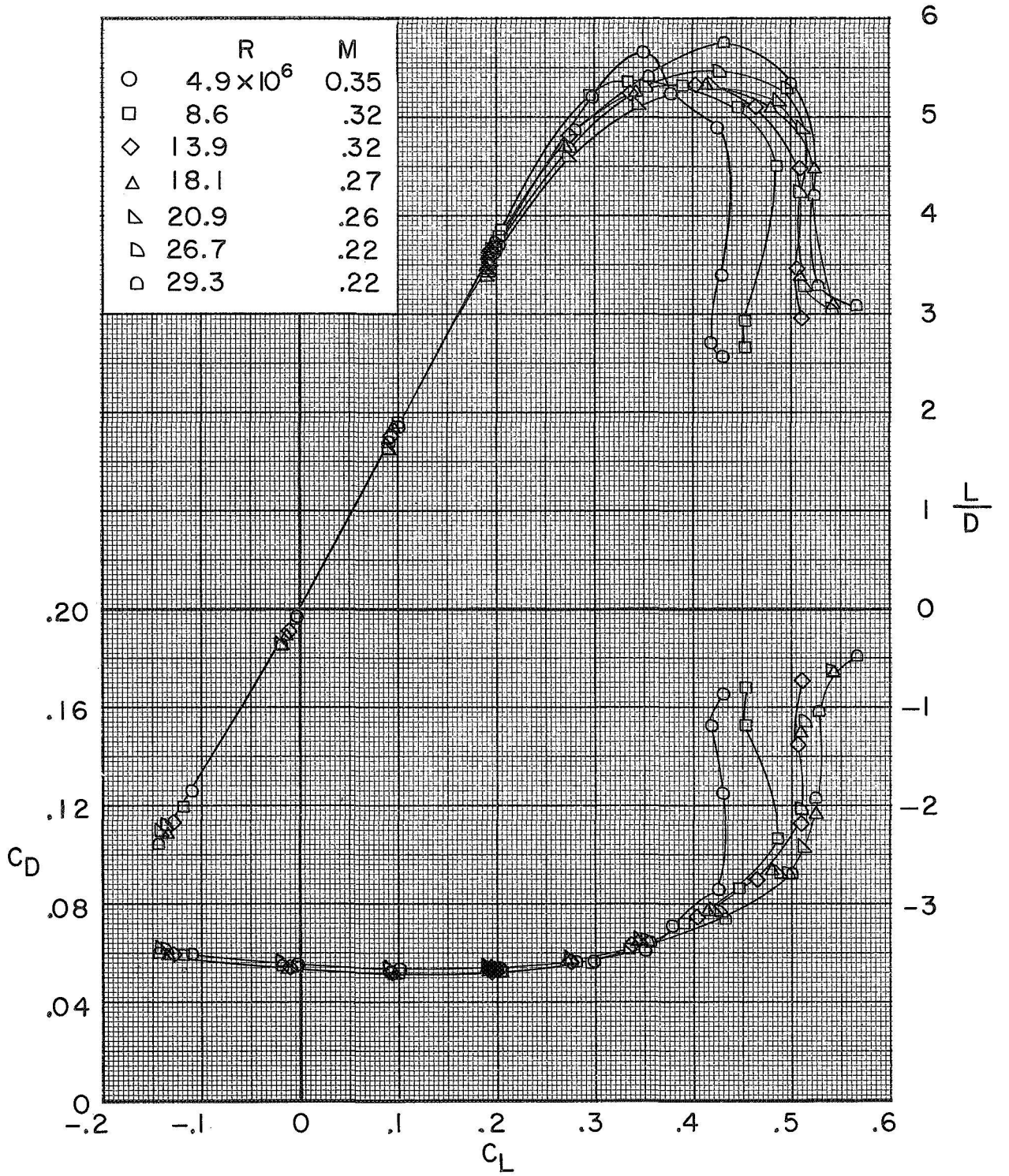

Figure 6.- Concluded.

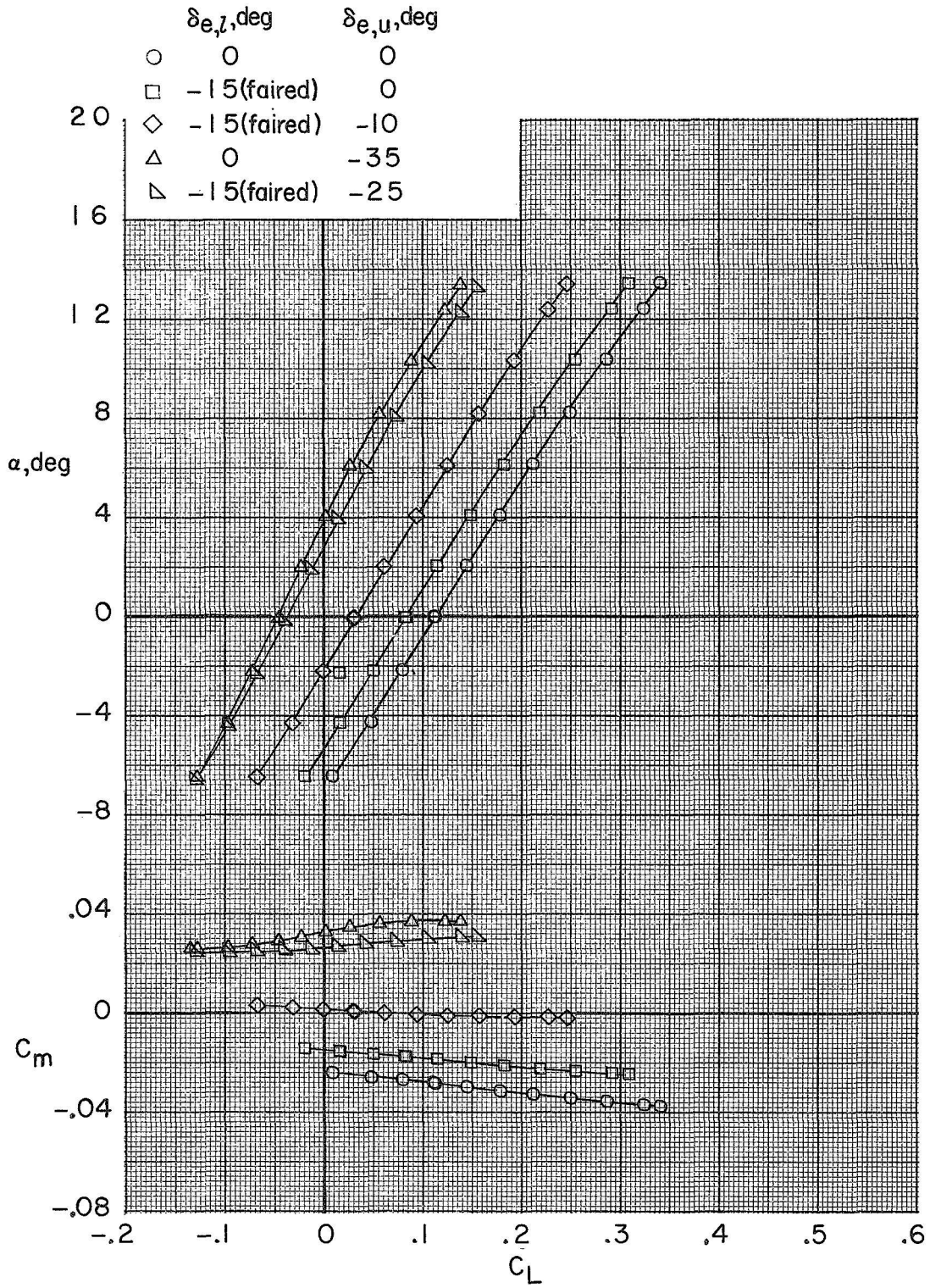

Figure 7.- Effect of elevon deflections on the longitudinal aerodynamic characteristics of the model with wings stowed ($\Lambda = 90^{o}$). $R = 13.5 \times 10^{6}$; $M = 0.32$.

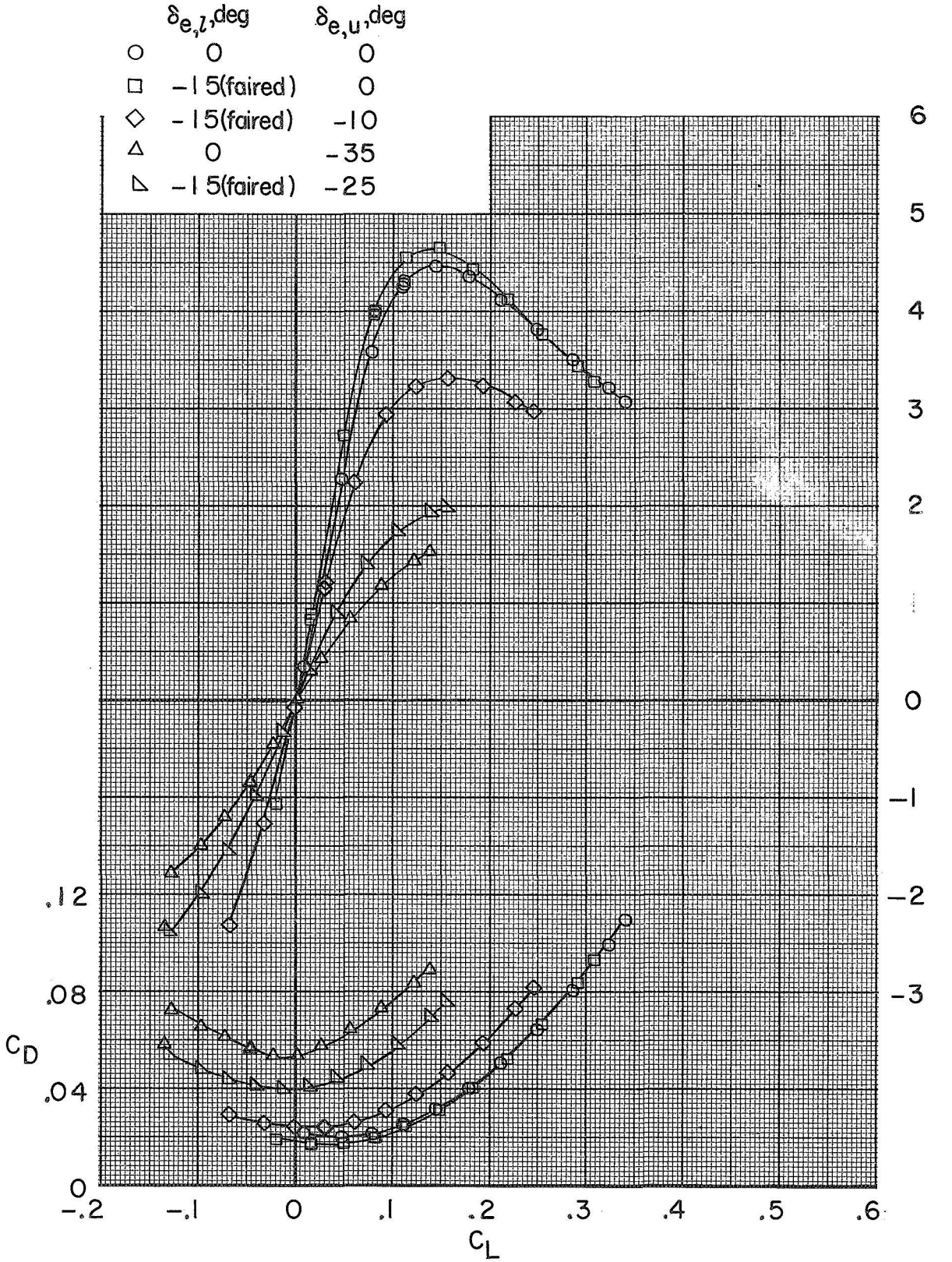

Figure 7.- Concluded.

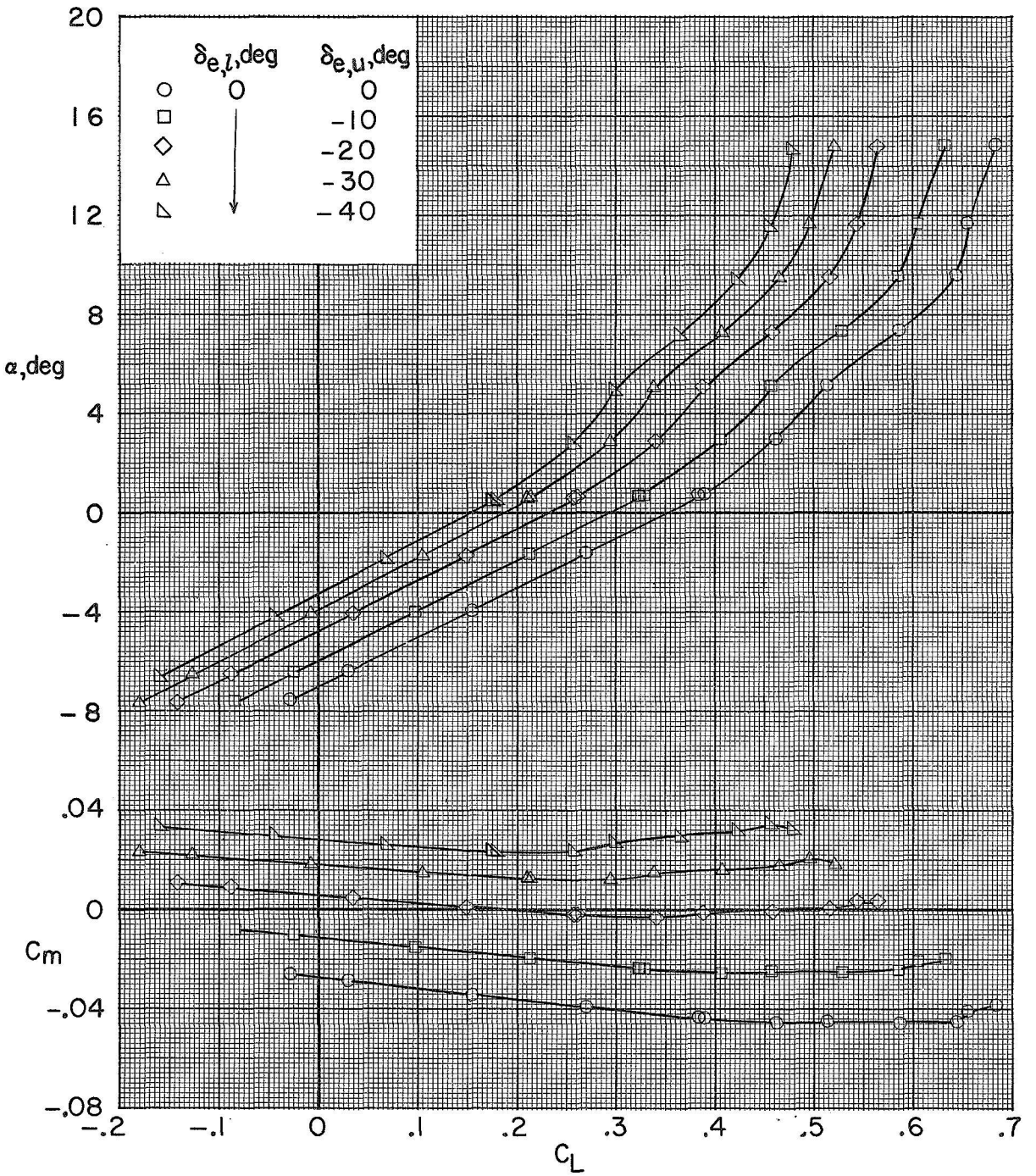

(a) $\delta_{e,l} = 0^0$.

Figure 8.- Effect of elevon deflections on the longitudinal aerodynamic characteristics of the model with the wings deployed to $\Lambda = 20^0$. $R = 14.8 \times 10^6$; $M = 0.32$.

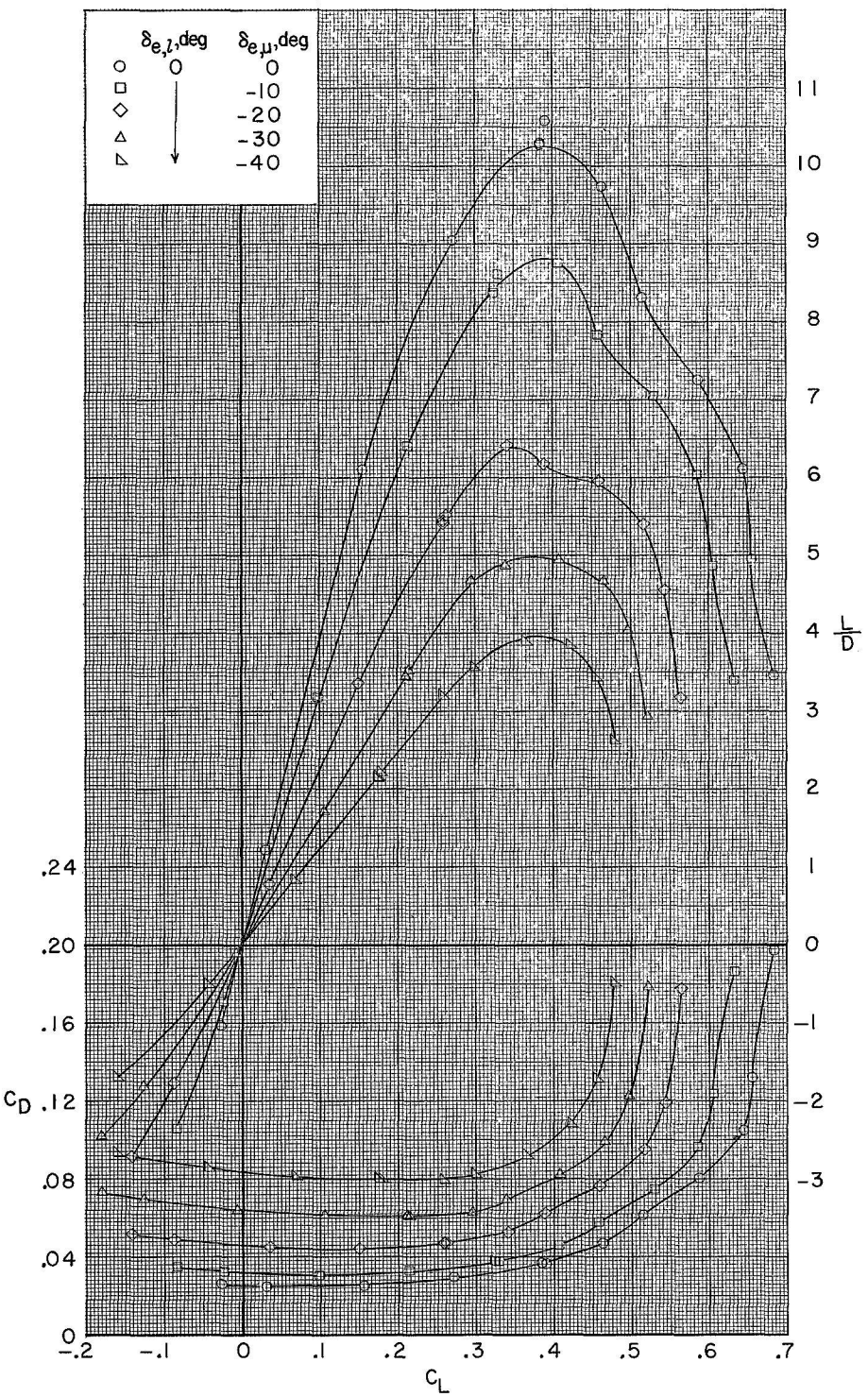

(a) $\delta_{e,l} = 0^0$. Concluded.

Figure 8.- Continued.

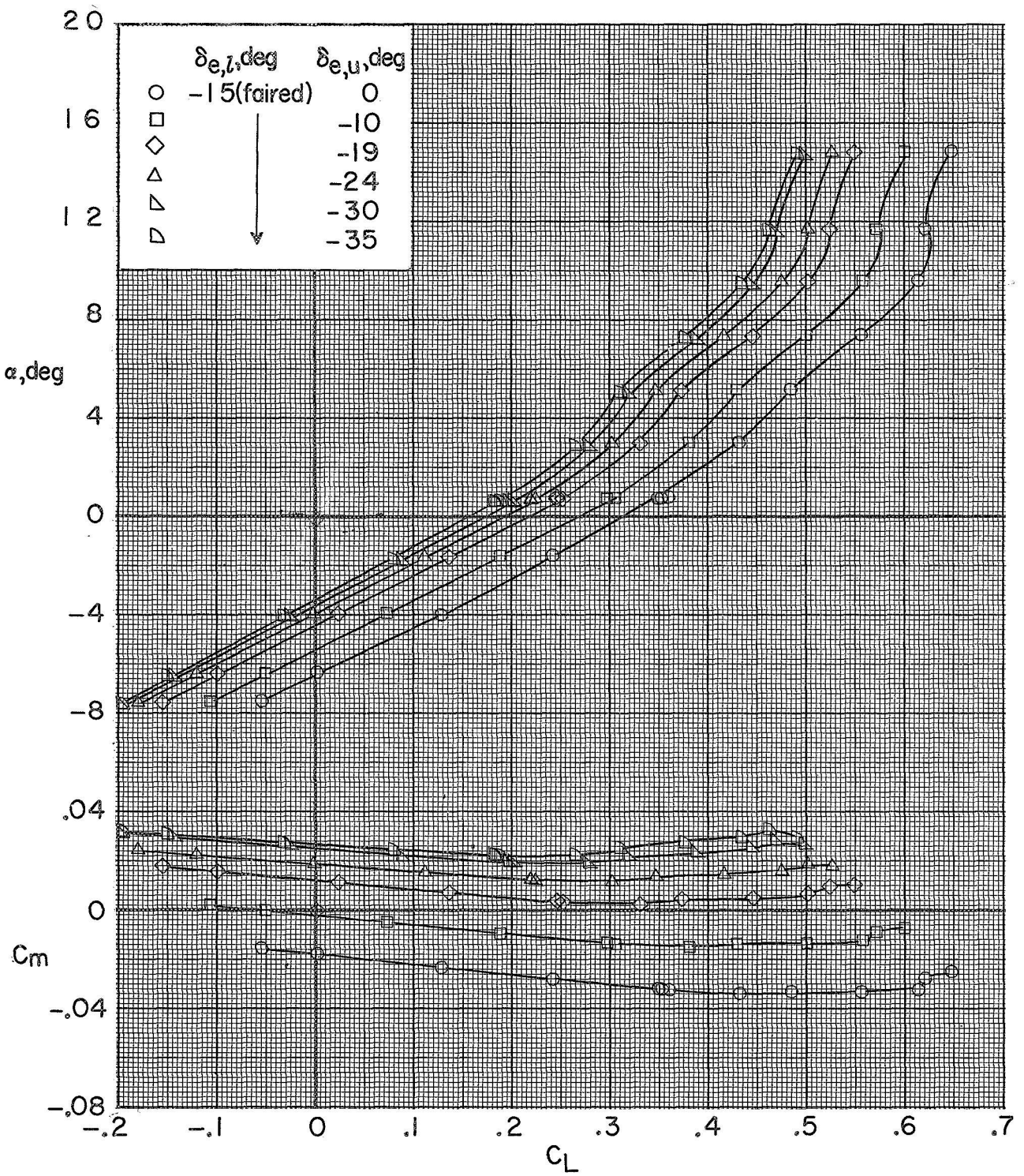

(b) $\delta_{e,l} = -15^{0}$ (faired).

Figure 8.- Continued.

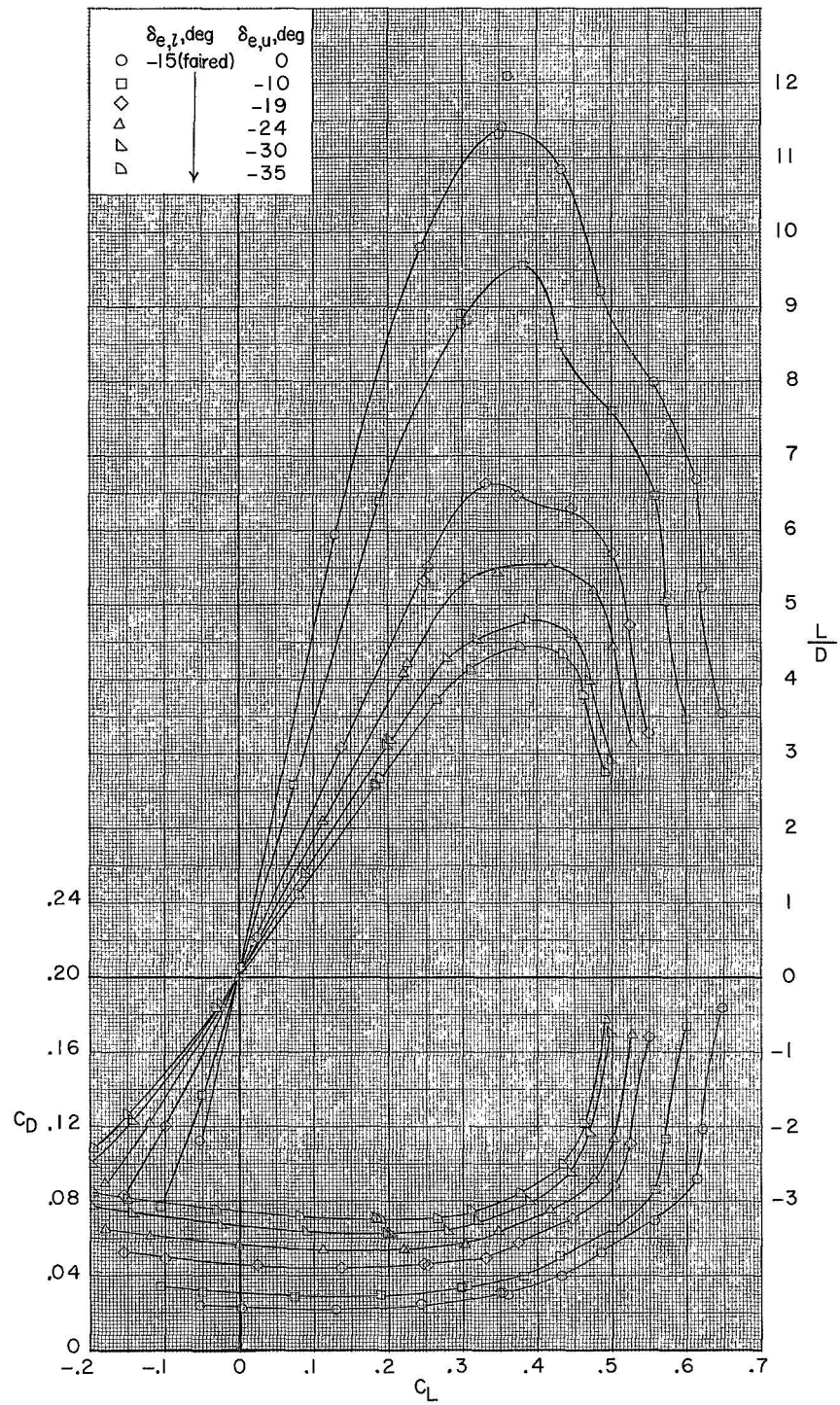

(b) $\delta_{e,l} = -15^0$ (faired). Concluded.

Figure 8.- Concluded.

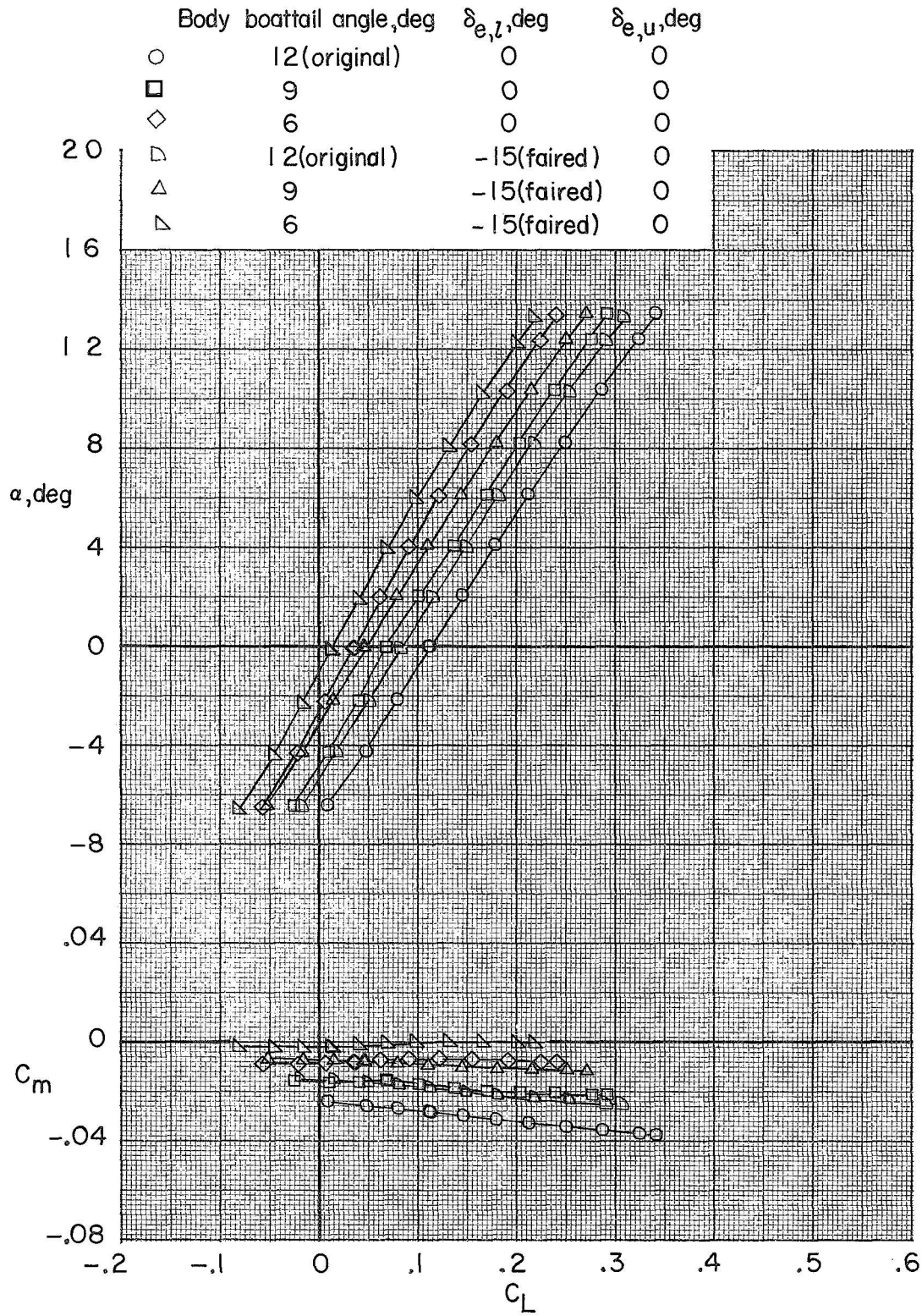

Figure 9.- Effect of reduced body boattail on the longitudinal aerodynamic characteristics of the model with wings stowed ($\Lambda = 90^{o}$). $R = 13.5 \times 10^{6}$; $M = 0.32$.

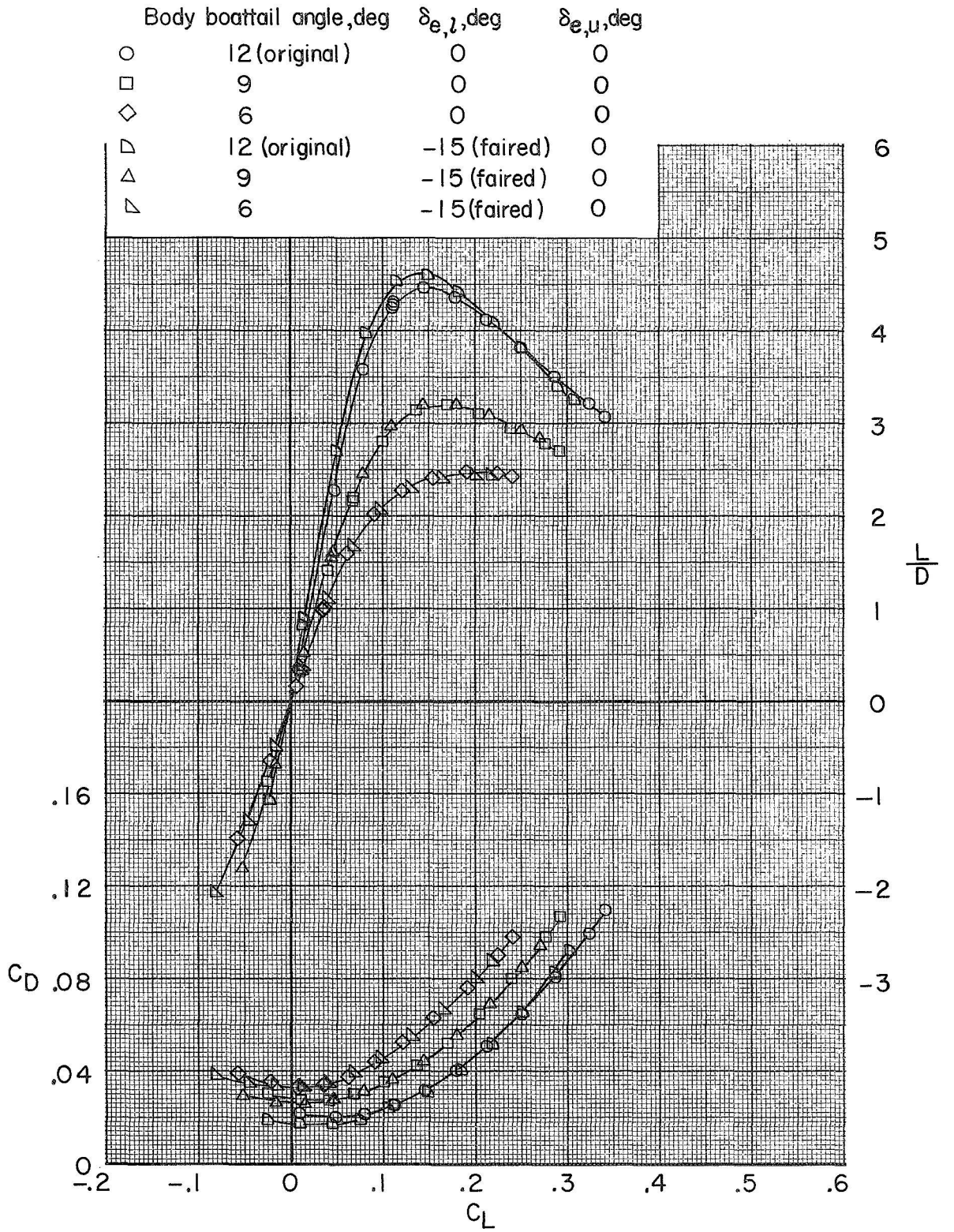

Figure 9.- Concluded.

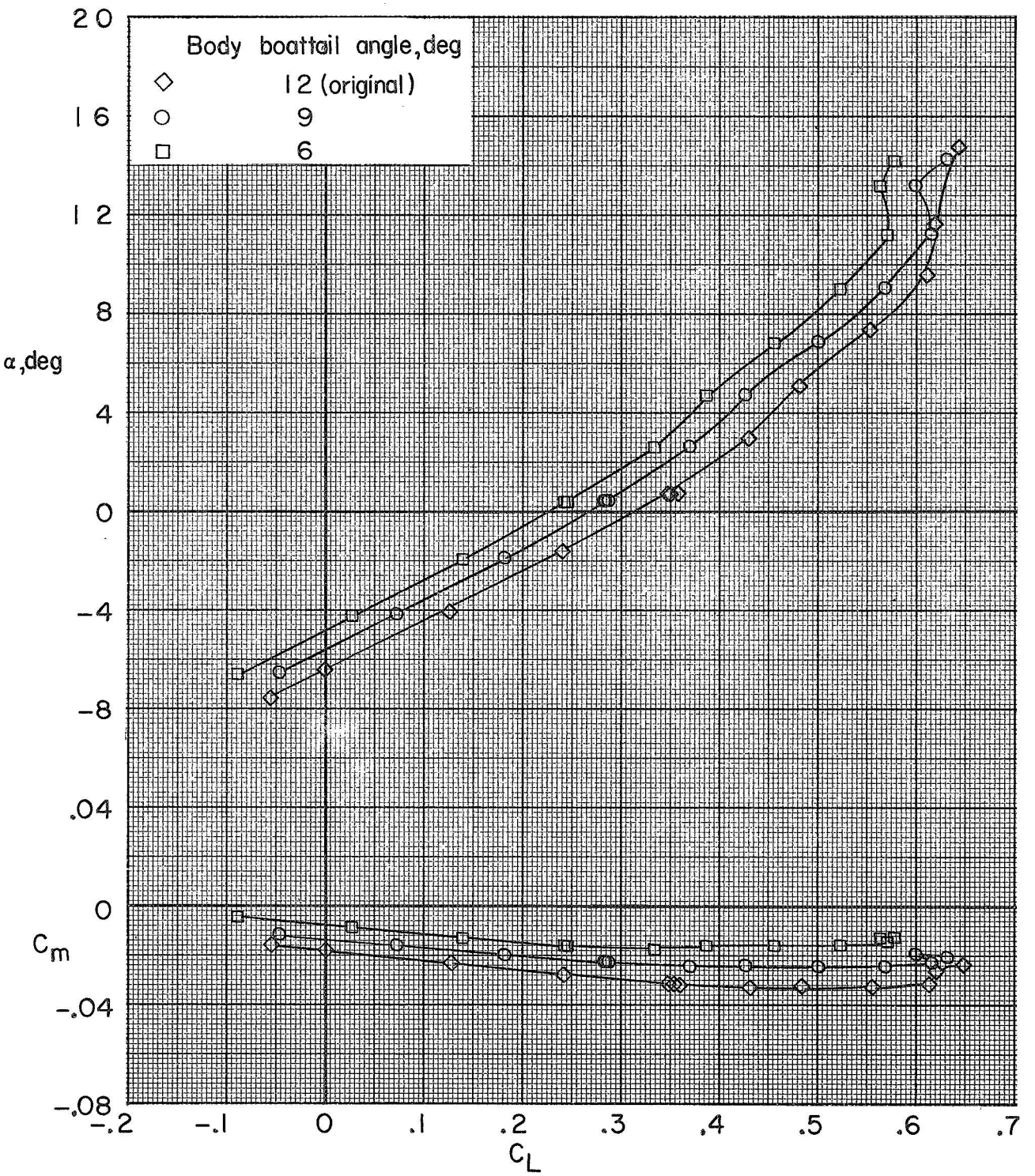

Figure 10.- Effect of reduced body boattail on the longitudinal aerodynamic characteristics of the model with wings deployed to $\Lambda = 20^0$. $R = 13.5 \times 10^6$; $\delta_{e,l} = -15^0$ (faired); $\delta_{e,u} = 0^0$; $M = 0.32$.

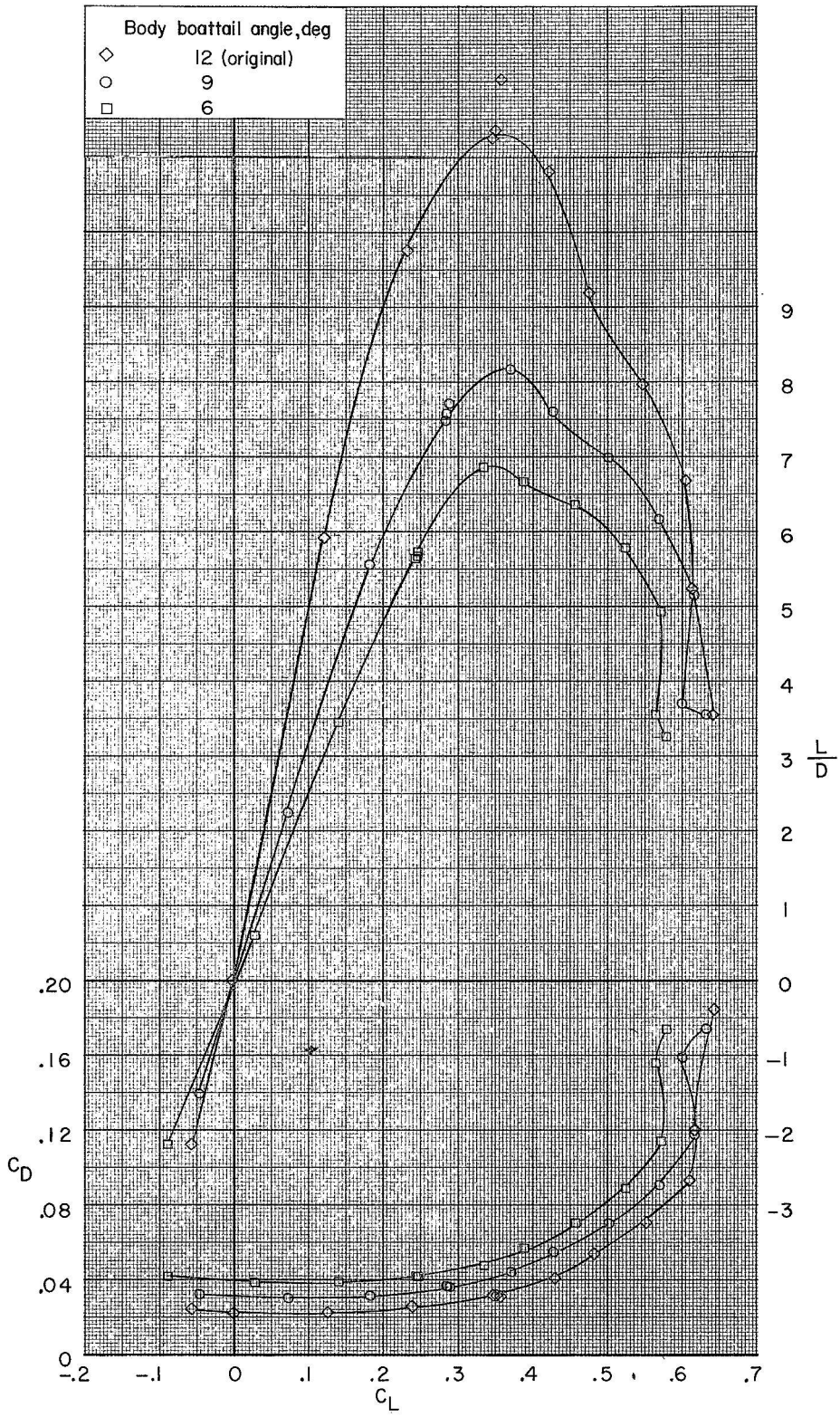

Figure 10.- Concluded.

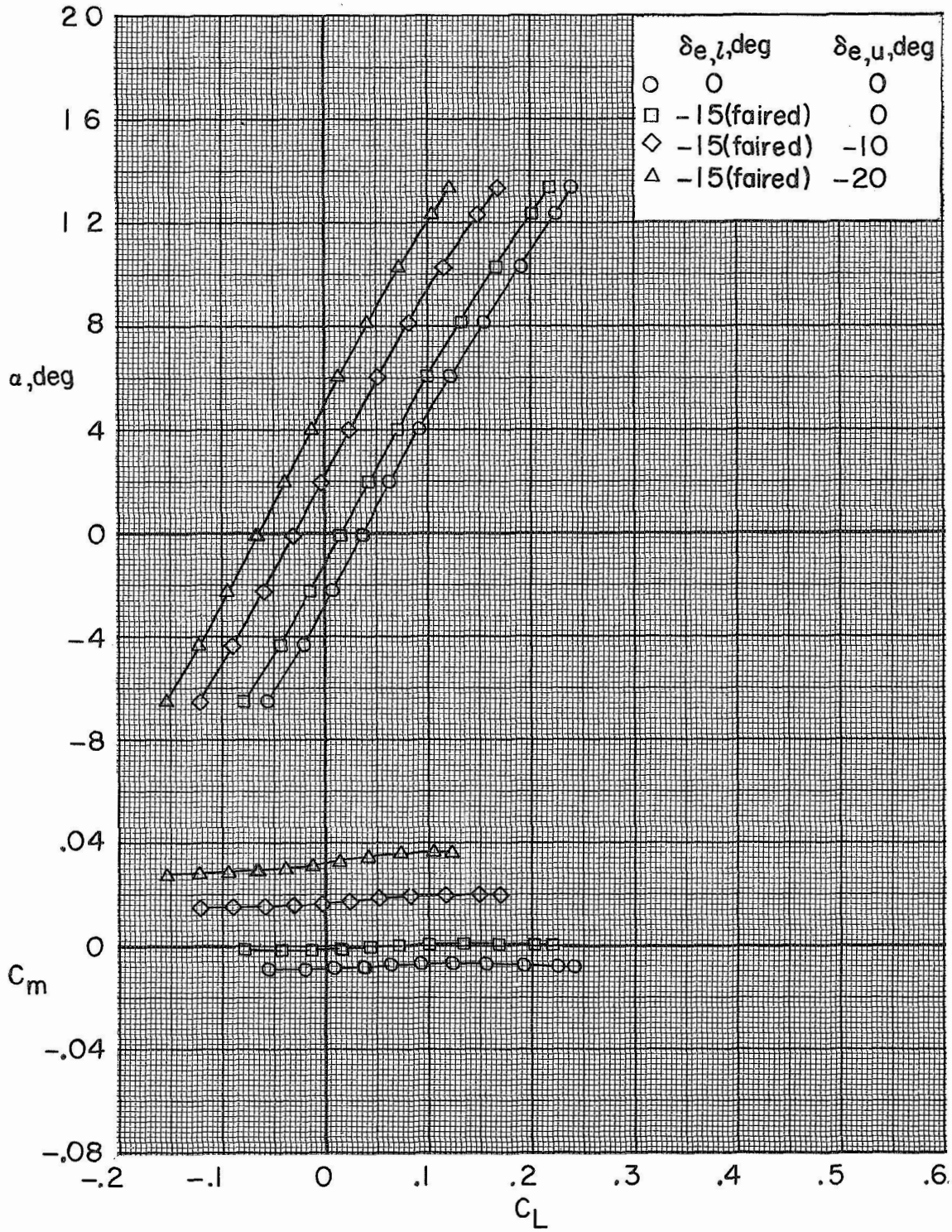

Figure 11.- Effect of elevon deflections on the longitudinal aerodynamic characteristics of a configuration with a body boattail angle of 6^0 and with wings stowed ($\Lambda = 90^0$). $R = 13.5 \times 10^6$; $M = 0.32$.

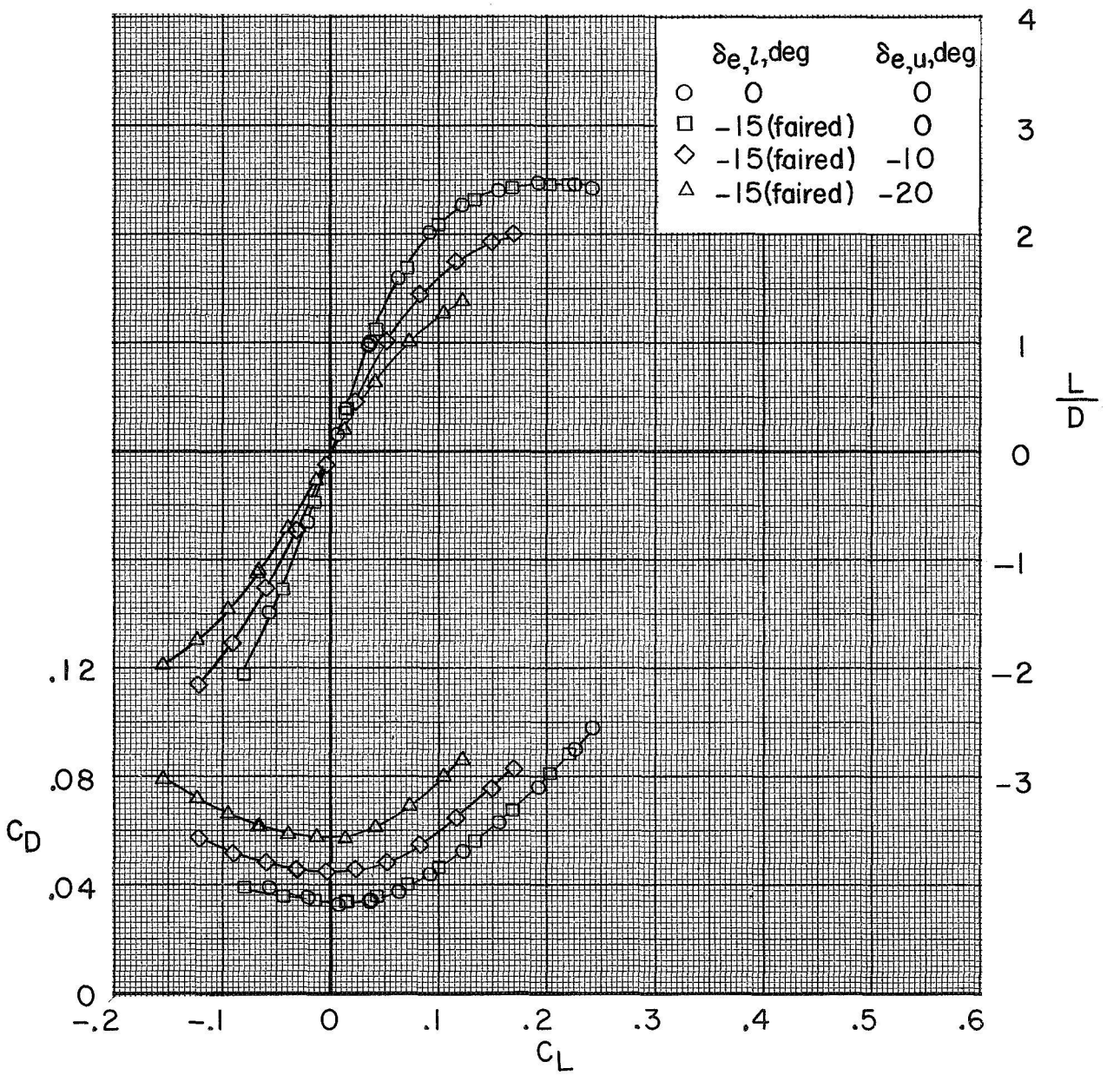

Figure 11.- Concluded.

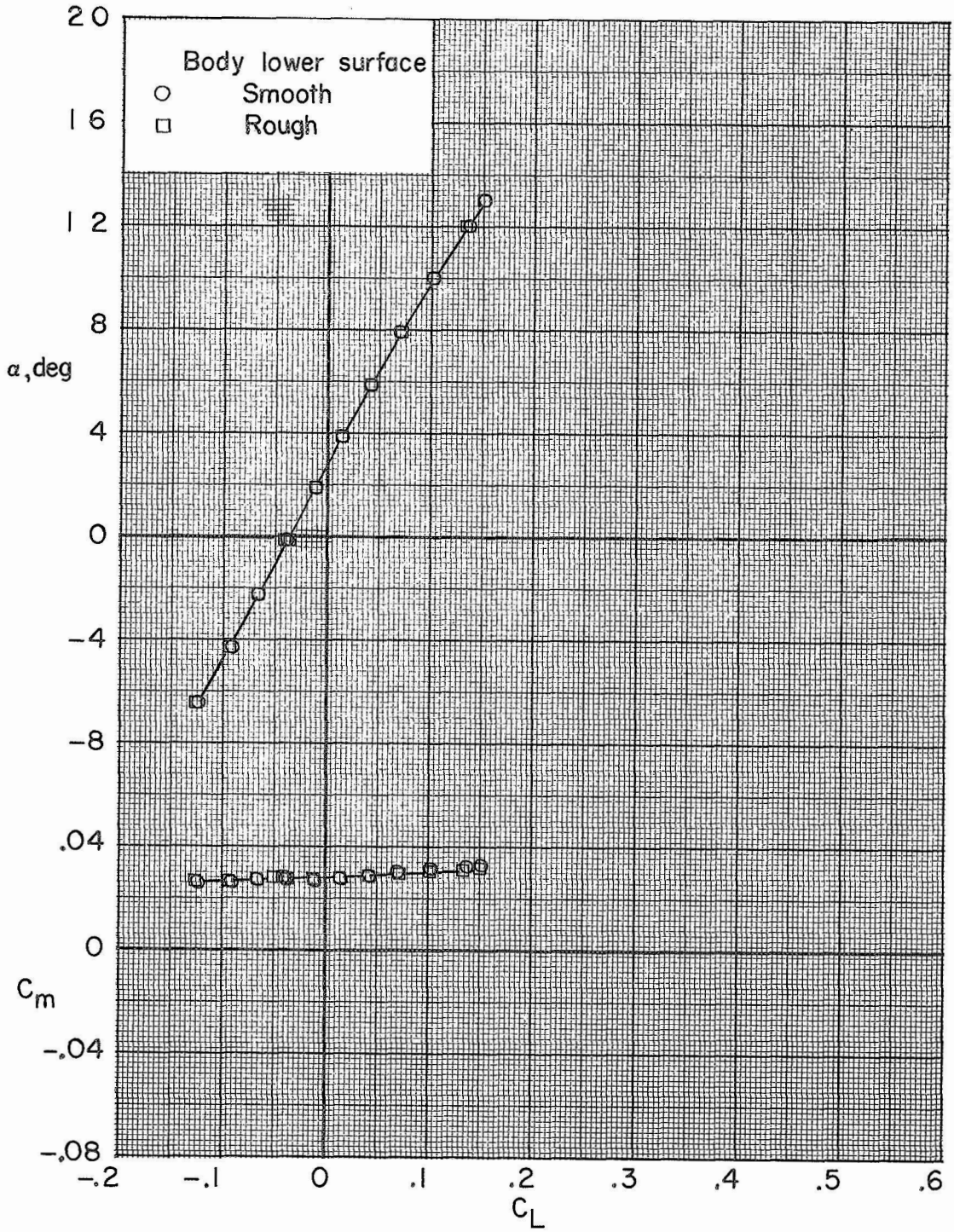

(a) R = 5.5 × 10^6; M = 0.41.

Figure 12.- Effect of simulated ablative roughness on the longitudinal aerodynamic characteristics of the model with wing stowed ($\Lambda = 90^0$). $\delta_{e,l} = -15^0$ (faired); $\delta_{e,u} = -25^0$.

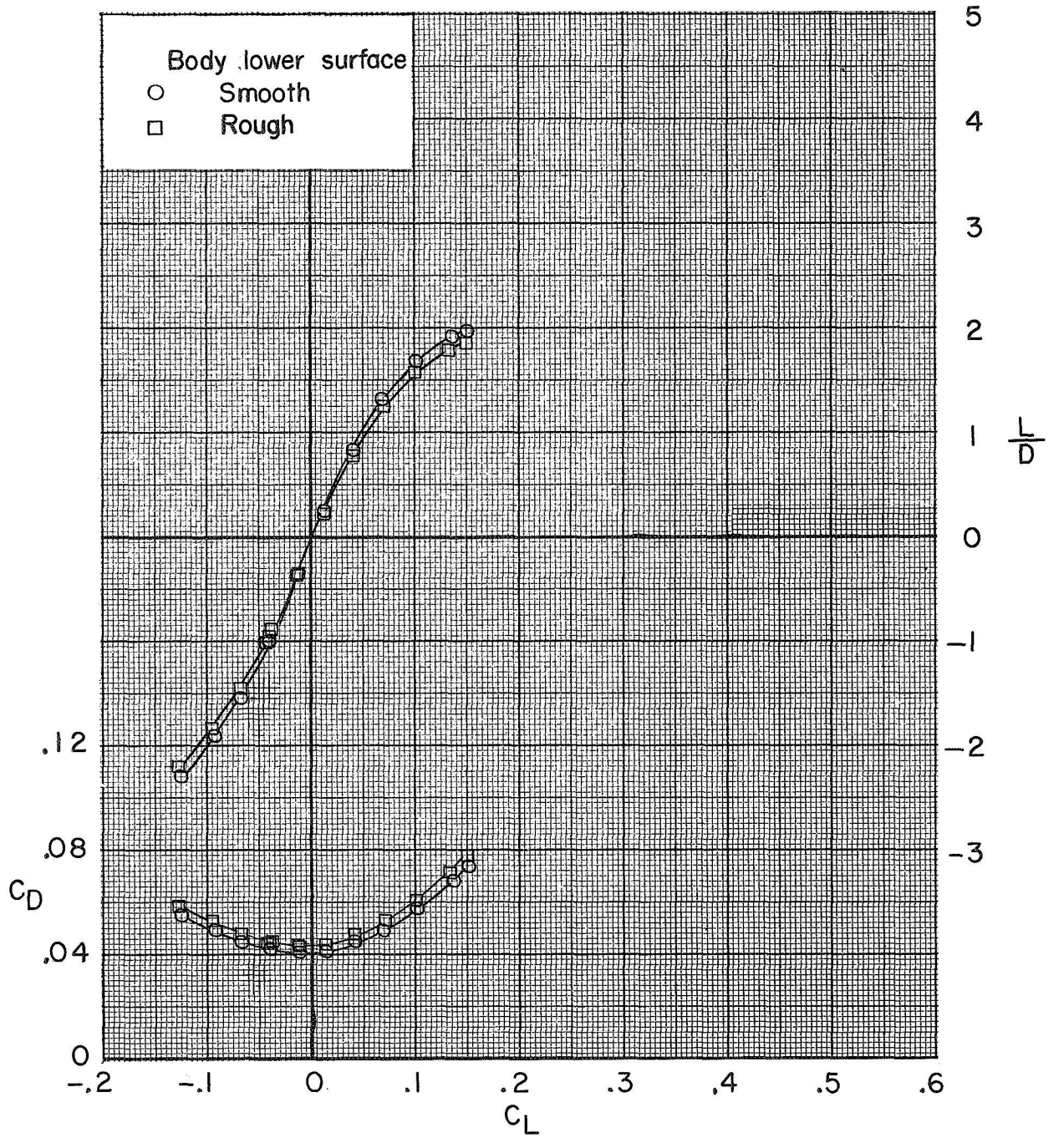

(a) R = 5.5 × 10^6; M = 0.41. Concluded.

Figure 12.- Continued.

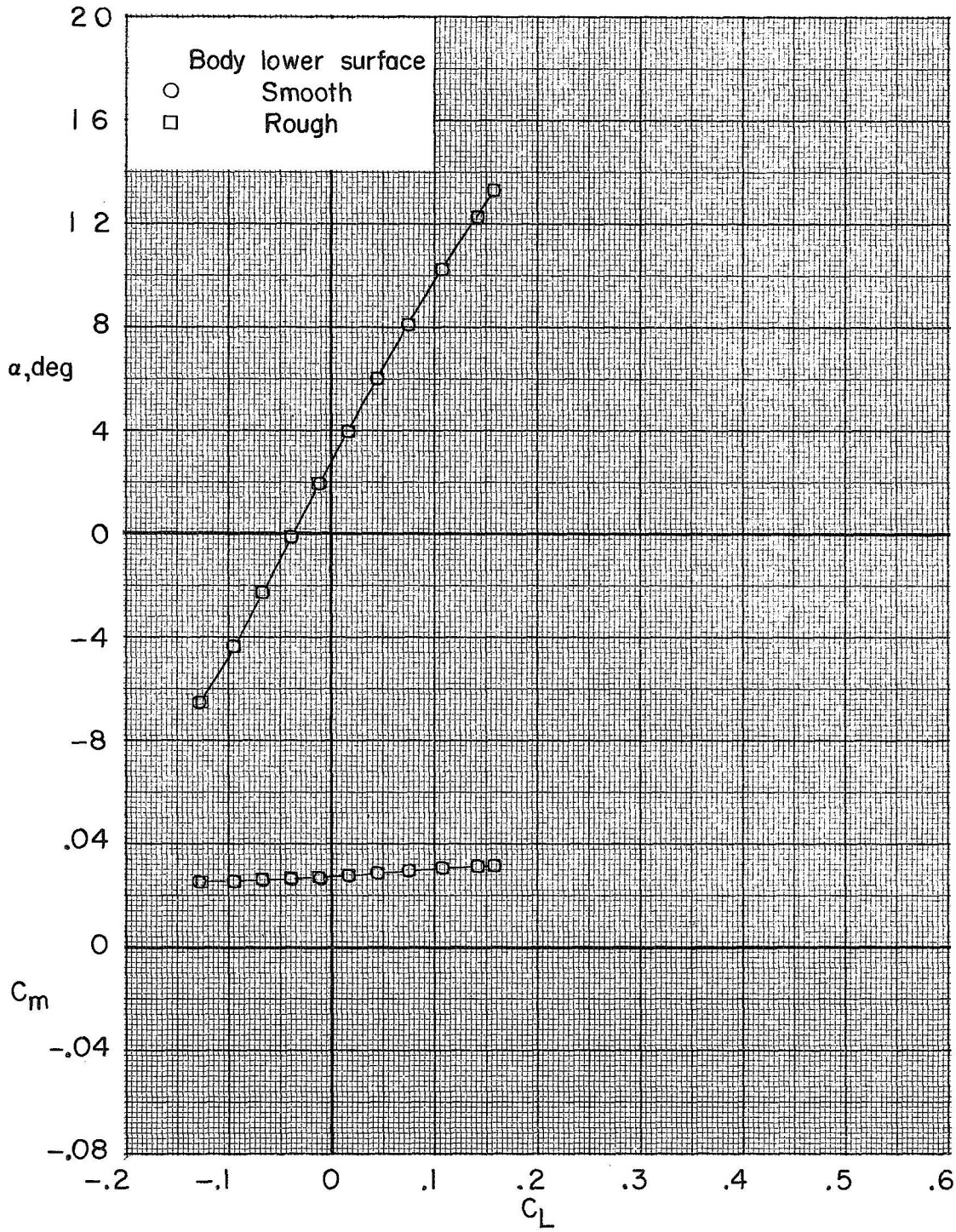

(b) R = 13.5 × 10^6; M = 0.32.

Figure 12.- Continued.

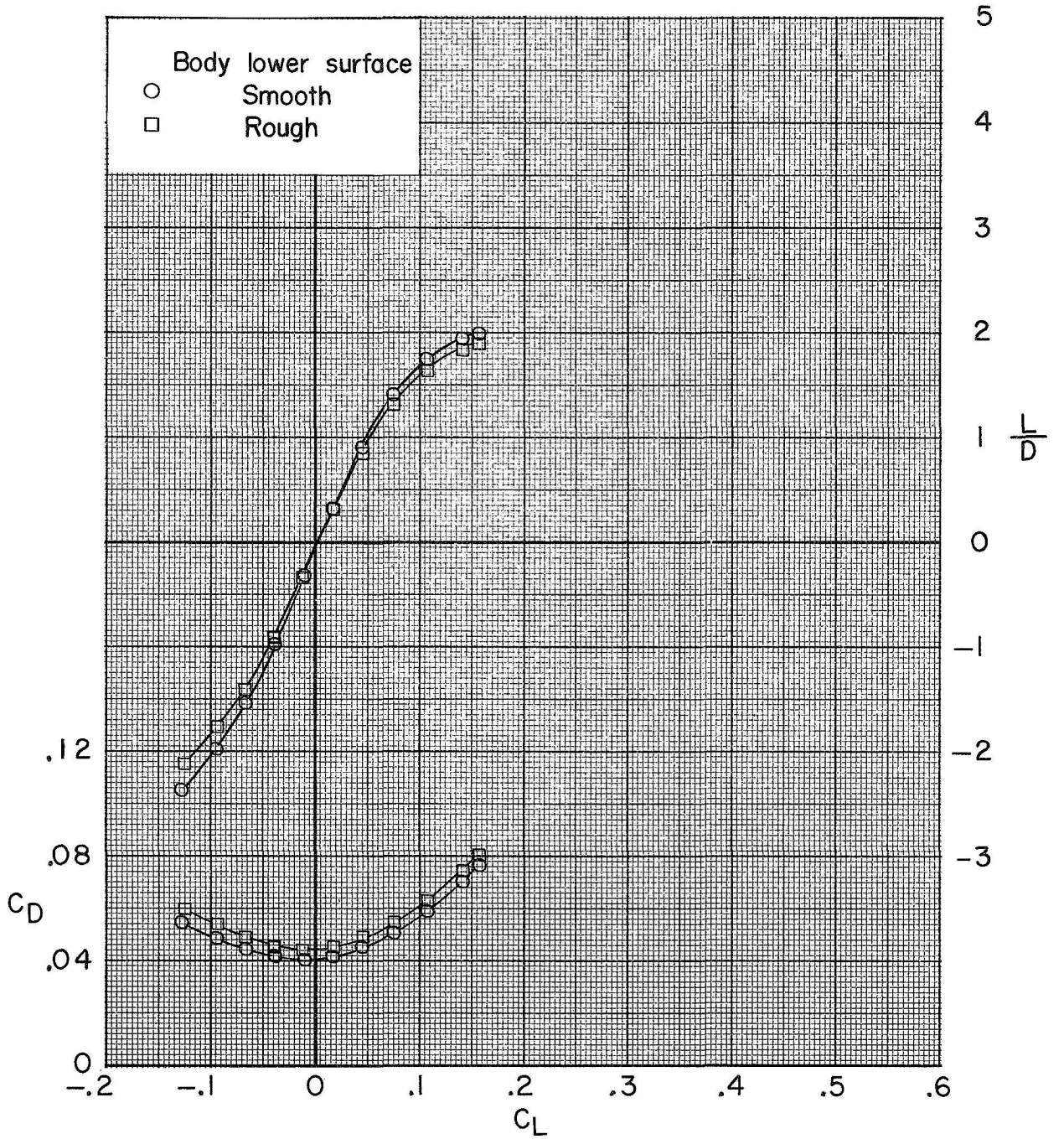

(b) R = 13.5 × 10^6; M = 0.32. Concluded.

Figure 12.- Continued.

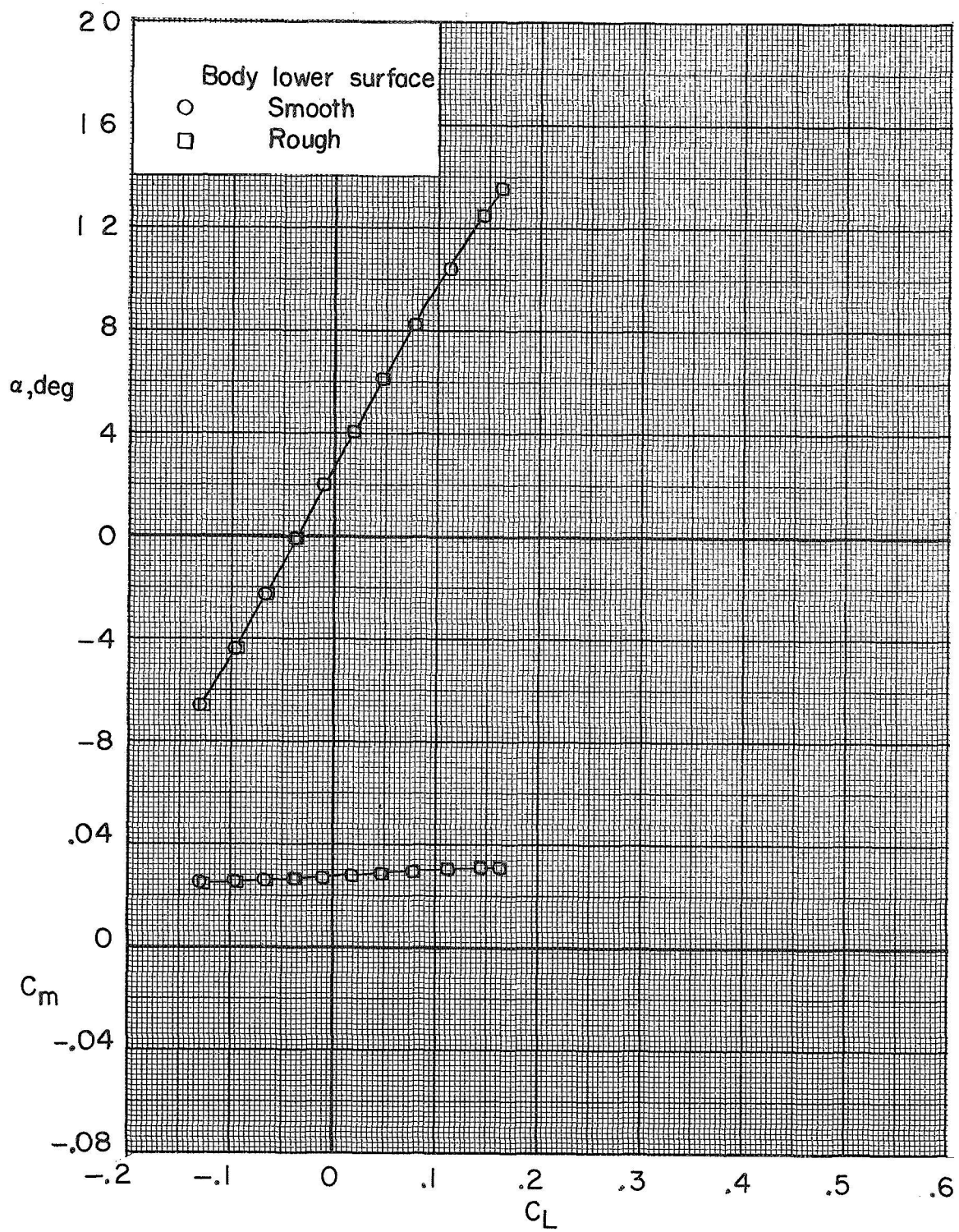

(c) R = 22.2 × 10⁶; M = 0.24.

Figure 12.- Continued.

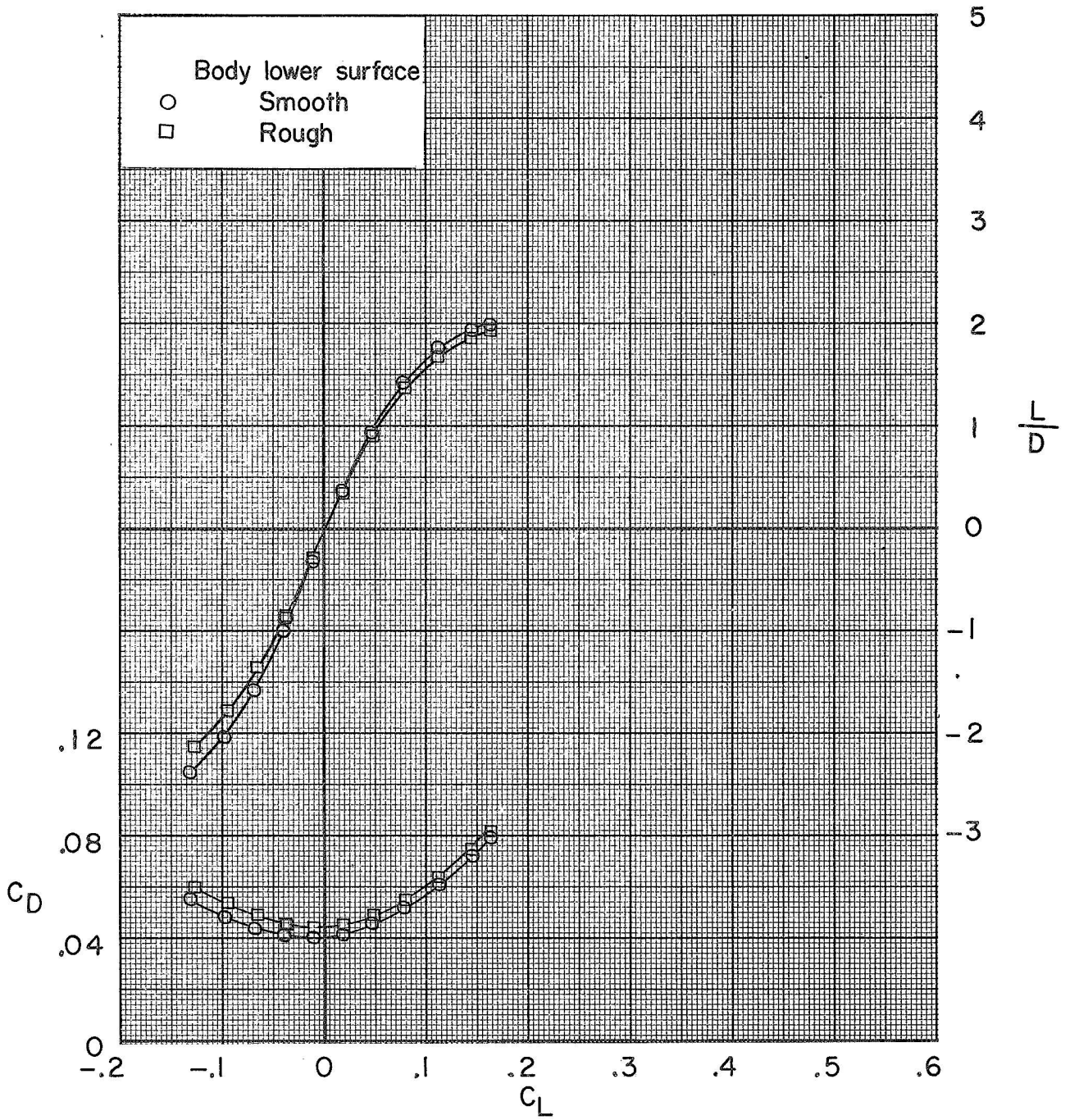

(c) R = 22.2 × 10^6; M = 0.24. Concluded.

Figure 12.- Continued.

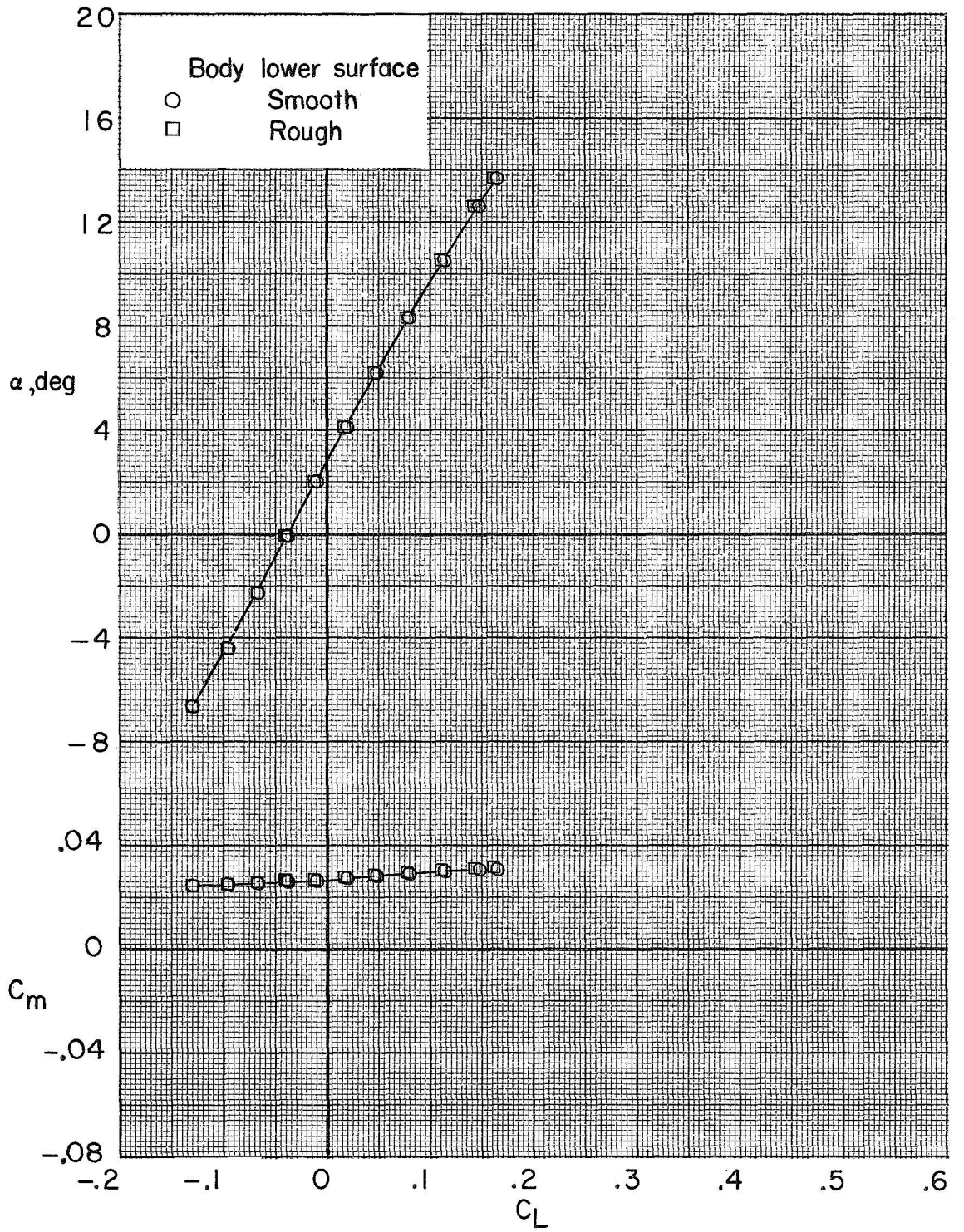

(d) $R = 29.5 \times 10^6$; $M = 0.21$.

Figure 12.- Continued.

NATIONAL AERONAUTICS AND SPACE ADMINISTRATION
WASHINGTON, D.C. 20546

OFFICIAL BUSINESS

FIRST CLASS MAIL

POSTAGE AND FEES PAID
NATIONAL AERONAUTICS AN
SPACE ADMINISTRATION

POSTMASTER: If Undeliverable (Section 158 Postal Manual) Do Not Return

"The aeronautical and space activities of the United States shall be conducted so as to contribute . . . to the expansion of human knowledge of phenomena in the atmosphere and space. The Administration shall provide for the widest practicable and appropriate dissemination of information concerning its activities and the results thereof."

—NATIONAL AERONAUTICS AND SPACE ACT OF 1958

NASA SCIENTIFIC AND TECHNICAL PUBLICATIONS

TECHNICAL REPORTS: Scientific and technical information considered important, complete, and a lasting contribution to existing knowledge.

TECHNICAL NOTES: Information less broad in scope but nevertheless of importance as a contribution to existing knowledge.

TECHNICAL MEMORANDUMS: Information receiving limited distribution because of preliminary data, security classification, or other reasons.

CONTRACTOR REPORTS: Scientific and technical information generated under a NASA contract or grant and considered an important contribution to existing knowledge.

TECHNICAL TRANSLATIONS: Information published in a foreign language considered to merit NASA distribution in English.

SPECIAL PUBLICATIONS: Information derived from or of value to NASA activities. Publications include conference proceedings, monographs, data compilations, handbooks, sourcebooks, and special bibliographies.

TECHNOLOGY UTILIZATION PUBLICATIONS: Information on technology used by NASA that may be of particular interest in commercial and other non-aerospace applications. Publications include Tech Briefs, Technology Utilization Reports and Notes, and Technology Surveys.

Details on the availability of these publications may be obtained from:

SCIENTIFIC AND TECHNICAL INFORMATION DIVISION

NATIONAL AERONAUTICS AND SPACE ADMINISTRATION

Washington, D.C. 20546